Cell. Mol. Life Sci. 63 (2006) 2039–2056
1420-682X/06/172039-18
DOI 10.1007/s00018-006-6208-2

Cellular and Molecular Life Sciences

Research Article

Chronic gestational exposure to ethanol causes insulin and IGF resistance and impairs acetylcholine homeostasis in the brain

S. J. Soscia, M. Tong, X. J. Xu, A. C. Cohen, J. Chu, J. R. Wands and S. M. de la Monte*

Departments of Pathology and Medicine, Pierre Galletti Research Building, Rhode Island Hospital, Brown Medical School,, 55 Claverick Street, Room 419, Providence, RI 02903 (USA), Fax: +1 401 444 2939, e-mail: Suzanne_DeLaMonte_MD@Brown.edu

Received 4 May 2006; received after revision 13 June 2006; accepted 20 June 2006
Online First 11 August 2006

Abstract. In fetal alcohol syndrome (FAS), cerebellar hypoplasia is associated with impaired insulin-stimulated survival signaling. This study characterizes ethanol dose-effects on cerebellar development, expression of genes required for insulin and insulin-like growth factor (IGF) signaling, and the upstream mechanisms and downstream consequences of impaired signaling in relation to acetylcholine (ACh) homeostasis. Pregnant Long Evans rats were fed isocaloric liquid diets containing 0%, 2%, 4.5%, 6.5%, or 9.25% ethanol from gestation day 6. Ethanol caused dose-dependent increases in severity of cerebellar hypoplasia, neuronal loss, proliferation of astrocytes and microglia, and DNA damage. Ethanol also reduced insulin, IGF-I, and IGF-II receptor binding, insulin and IGF-I receptor tyrosine kinase activities, ATP, membrane cholesterol, and choline acetyltransferase (ChAT) expression. *In vitro* studies linked membrane cholesterol depletion to impaired insulin receptor binding and insulin-stimulated ChAT. In conclusion, cerebellar hypoplasia in FAS is mediated by insulin/IGF resistance with attendant impairments in energy production and ACh homeostasis.

Keywords. Ethanol, fetal alcohol syndrome, insulin resistance, insulin-like growth factor, receptor binding affinity, membrane cholesterol, acetylcholine.

Introduction

Ethanol exposure during development is the leading preventable cause of mental retardation in Europe and North America. Heavy or chronic gestational exposure to ethanol causes fetal alcohol syndrome (FAS), which encompasses a broad array of neurological and systemic lesions including central nervous system (CNS) malformations such as microencephaly, reduced cerebral white matter volume, ventriculomegaly, cerebellar hypoplasia, and disorders of neuronal migration [1, 2]. However, much less is known about the full range of human CNS disease produced by lower levels of ethanol exposure due to the lack of accurate clinicopathological correlative data. Experimental models of FAS have provided insight about the range of ethanol-induced CNS abnormalities by demonstrating that gestational exposure to ethanol impairs neuronal survival, growth, migration, synaptogenesis, maturation, neurotransmitter function, and intracellular adhesion [3–8]. In addition, experimental models of FAS have provided evidence that ethanol can exert neurotoxic effects on the developing CNS, even after relatively short durations or low levels of exposure [3]. Therefore, with regard to human beings, there is concern that low or moderate levels of *in utero* ethanol exposure can have significant adverse effects on the developing brain, and may be

* Corresponding author.

responsible for the growing incidence of attention deficit/hyperactivity disorders [9–11].

Neuronal genesis, differentiation, and migration are critical on-going processes likely to be perturbed by gestational exposure to ethanol. In the developing CNS, insulin, insulin-like growth factor type 1 (IGF-1), and IGF-II receptors are abundantly expressed [12–14], and their corresponding growth factors mediate neuronal growth, survival, energy metabolism, and synapse formation. In addition, there is growing evidence that insulin and IGF signaling mechanisms are key targets of ethanol-mediated neurotoxicity in the immature CNS [15–18]. Neuronal loss that is associated with ethanol-induced microencephaly is mediated by inhibition of insulin/IGF-1-stimulated survival signaling [15, 16, 19, 20], and attendant increased apoptosis [15, 16, 21] and mitochondrial dysfunction [16, 19, 20, 22].

Recent studies designed to divulge the mechanisms of ethanol-impaired insulin/IGF signaling in the developing brain demonstrated that chronic gestational exposure to relatively high levels of ethanol inhibit insulin gene expression, but produce only modest alterations in the expression of insulin and IGF-I receptors [23]. Although those results suggest that cell loss in ethanol-exposed developing brains may be mediated by a local deficiency of brain-derived insulin, the finding of reduced levels of insulin and IGF-I receptor tyrosine kinase activities following exogenous growth factor stimulation, suggests additional abnormalities contribute to the impairments in CNS development. Moreover, *in vitro* experiments demonstrated ethanol inhibition of IGF-I and IGF-II, but not insulin receptor expression, yet insulin and IGF-I stimulated glucose uptake and ATP synthesis were similarly impaired [23]. Therefore, the mechanisms by which ethanol adversely affects insulin and IGF-I responsiveness in neurons require further investigation. We now present data showing dose-dependent effects of chronic gestational exposure to ethanol on CNS: (1) development; (2) insulin, IGF-1, and IGF-II receptor binding; (3) ATP levels; and (4) choline acetyltransferase (ChAT) expression in the cerebellum. Importantly, these observations link ethanol-mediated insulin and IGF resistance in the CNS to deficits in acetylcholine homeostasis, which could account for many of the cognitive-motor deficits observed in FAS.

Materials and methods

***In vivo* model of chronic ethanol exposure.** Pregnant Long-Evans rats were fed with isocaloric liquid diets (BioServ, Frenchtown, N.J.) in which ethanol comprised 0%, 2%, 4.5%, 6.5%, 9.25% (v/v), which is equivalent to 0%, 8%, 18%, 26%, or 37% of the caloric content. These concentrations of ethanol are typically used to generate *in vivo* models of chronic ethanol exposure [24]. The liquid diets were begun on gestation day 6 and continued throughout pregnancy. Rats were monitored daily to ensure equivalent caloric consumption and maintenance of body weight. Since the cerebellum represents a major target of ethanol neurotoxicity [3, 25, 26], cerebella were used to study the effects of chronic gestational exposure to ethanol on insulin and IGF signaling in the developing CNS. Fresh tissue harvested immediately after birth was snap frozen in a dry ice-methanol bath and then stored at –80 °C for mRNA and protein studies. In addition, cerebella were immersion fixed in Histochoice fixative (Amresco Corp., Solon, OH) and embedded in paraffin. Histological sections were stained with hematoxylin and eosin (H&E) and examined by light microscopy.

Immunohistochemical staining: Paraffin-embedded sections (8 μm thick) of cerebellar tissue were immunostained with monoclonal anti-single-stranded DNA antibody (Chemicon International., Temecula, CA). Prior to immunostaining, the deparaffinized, re-hydrated tissue sections were sequentially treated with 0.1 mg/ml saponin in phosphate-buffered saline (10 mM sodium phosphate, 0.9% NaCl, pH 7.4; PBS), for 20 min at room temperature, followed by proteinase K digestion (20 μg/ml in PBS for 20 min at room temperature), and denaturation in 50% formamide/PBS at 60 °C for 20 min, according to the manufacturer's protocol. Endogenous peroxidase activity was quenched by treating the tissue sections with 3% hydrogen peroxide in methanol for 10 min, and non-specific binding sites were blocked by a 30-min incubation in SuperBlock-TBS (Pierce Chemical Co., Rockford, IL) at room temperature. After overnight incubation at 4 °C with 2 μg/ml FT-26 antibody to single-stranded DNA, immunoreactivity was detected using biotinylated secondary antibody, avidin biotin horseradish peroxidase complex (ABC) reagents, and diaminobenzidine (DAB) as the chromogen (Vector Laboratories, Burlingame, CA) [27]. The sections were counterstained with hematoxylin and examined by light microscopy.

Real-time quantitative RT-PCR assays. Total RNA was isolated from cerebellar tissue using TRIzol reagent (Invitrogen, Carlsbad, CA) according to the manufacturer's protocol. RNA concentrations were determined from the absorbances measured at 260 nm, and purity was judged from the 260/280 nm ratios. RNA (2 μg) was reverse transcribed using the AMV First Strand cDNA synthesis kit (Roche Diagnostics Corporation, Indianapolis, IN) and random oligodeoxynucleotide primers. The mRNA levels of insulin, IGF-I, and IGF-II growth factors, their corresponding receptors, neuronal (Hu), astrocytic (glial fibrillary acidic protein; GFAP), oligodendroglial (myelin-associated glycoprotein-1; MAG-1), microglial (AIF1), and endothelial (endothelin-1; ET-1) cellular genes, acetyl-

cholinesterase (AChE), and ChAT were measured using real-time quantitative RT-PCR amplification. Ribosomal 18S RNA levels measured in parallel reactions were used to calculate relative abundance of each mRNA transcript [27, 28]. Ribosomal 28S RNA levels were also measured and the corresponding 28S/18S ratios were calculated to further assess RNA integrity. PCR amplifications were performed in 25-µl reactions containing cDNA generated from 2.5 ng original RNA template, 300 nM each of gene-specific forward and reverse primer (Table 1), and 12.5 µl 2 × QuantiTect SYBR Green PCR Mix (Qiagen Inc, Valencia, CA). The amplified signals were detected continuously with the Bio-Rad iCycler iQ Multi-Color RealTime PCR Detection System (Bio-Rad, Hercules, CA). The amplification protocol used was as follows: initial 15-min denaturation and enzyme activation at 95 °C, 40 cycles of 95 °C for 15 s, 55°–60 °C for 30 s, and 72 °C for 30 s. Annealing temperatures were optimized using the temperature gradient program provided with the iCycler software.

In preliminary studies, SYBR Green-labeled PCR products were evaluated by agarose gel electrophoresis, and the authenticity of each amplicon was verified by nucleic acid sequencing. The cDNAs were cloned into the PCRII vector (Invitrogen). Serial dilutions of known quantities of recombinant plasmid DNA containing the specific cDNA target sequences were used as standards in the PCR reactions, and the regression lines generated from the C_t values of the standards were used to calculate mRNA abundance. Relative mRNA abundance was determined from the nanogram ratios of specific mRNA to18S measured in the same samples [27, 28]. Results were normalized to 18S because 18S is highly abundant and the levels were essentially invariant among the samples, whereas housekeeping genes were found to be modulated with disease state. Inter-group statistical comparisons were made using the calculated mRNA/18S ratios. Control studies included real-time quantitative PCR analysis of: (1) template-free reactions; (2) RNA that had not been reverse transcribed; (3) RNA samples that were pre-treated with DNase I; (4) samples treated with RNase A prior to reverse transcriptase reaction; and (5) genomic DNA.

Receptor tyrosine kinase assays. Insulin or IGF-I receptor molecules were immunoprecipitated from individual 100 µg protein samples using rabbit polyclonal antibodies

Table 1. Primer pairs for real-time quantitative RT-PCR.

Primer	Direction	Sequence (5′→3′)	Position (mRNA)	Amplicon size (bp)
18S rRNA	For	GGA CAC GGA CAG GAT TGA CA	1278	50
18S rRNA	Rev	ACC CAC GGA ATC GAG AAA GA	1327	
28S rRNA	For	GGT AAA CGG CGG GAG TAA CTA TG	3712	107
28S rRNA	Rev	TAG GTA GGG ACA GTG GGA ATC TCG	3818	
Insulin	For	TTC TAC ACA CCC AAG TCC CGT C	145	135
Insulin	Rev	ATC CAC AAT GCC ACG CTT CTG C	279	
Insulin receptor	For	TGA CAA TGA GGA ATG TGG GGA C	875	129
Insulin receptor	Rev	GGG CAA ACT TTC TGA CAA TGA CTG	1003	
IGF-I	For	GAC CAA GGG GCT TTT ACT TCA AC	65	127
IGF-I	Rev	TTT GTA GGC TTC AGC GGA GCA C	191	
IGF-I receptor	For	GAA GTC TGC GGT GGT GAT AAA GG	2138	113
IGF-I receptor	Rev	TCT GGG CAC AAA GAT GGA GTT G	2250	
IGF-II	For	CCA AGA AGA AAG GAA GGG GAC C	763	95
IGF-II	Rev	GGC GGC TAT TGT TGT TCA CAG C	857	
IGF-II receptor	For	TTG CTA TTG ACC TTA GTC CCT TGG	1066	91
IGF-II Receptor	Rev	AGA GTG AGA CCT TTG TGT CCC CAC	1156	
AChE	For	TTC TCC CAC ACC TGT CCT CAT C	420	123
AChE	Rev	TTC ATA GAT ACC AAC ACG GTT CCC	542	
ChAT	For	TCA CAG ATG CGT TTC ACA ACT ACC	478	106
ChAT	Rev	TGG GAC ACA ACA GCA ACC TTG	583	
Hu	For	CAC TGT GTG AGG GTC CAT CTT CTG	271	50
Hu	Rev	TCA AGC CAT TCC ACT CCA TCT G	320	
GFAP	For	TGG TAA AGA CGG TGG AGA TGC G	1245	200
GFAP	Rev	GGC ACT AAA ACA GAA GCA AGG GG	1444	
MAG-1	For	AAC CTT CTG TAT CAG TGC TCC TCG	18	63
MAG-1	Rev	CAG TCA ACC AAG TCT CTT CCG TG	80	
ET-1	For	TTC CAA GAG AGG TTG AGG TGT TCC	957	83
ET-1	Rev	CAG CAA GAA GAG GCA AGA GAA TCA C	1039	
AIF-1	For	GGA TGG GAT CAA CAA GCA CT	168	158
AIF-1	Rev	GTT TCT CCA GCA TTC GCT TC	325	

RT-PCR = reverse transcriptase polymerase chain reaction; IGF-I = insulin-like growth factor, type I; AChE = acetylcholinesterase; ChAT = choline acetyltransferase; GFAP = glial fibrillary acidic protein; MAG-1 = myelin-associated glycoprotein; ET-1 = endothelin 1; AIF-1 = allograft inflammatory factor-1.

(1 µg/ml) and protein A Sepharose (Amersham-Pharmacia, Arlington Heights, IL) [29]. Receptor tyrosine kinase activity was measured in the immune precipitates using a non-isotopic assay (Chemicon International) according to the manufacturer's protocol with small modifications. Briefly, tyrosine phosphorylation of the biotinylated synthetic peptide substrate captured onto streptavidin-coated wells was detected with horseradish peroxidase conjugated anti-phospho-tyrosine and SuperSignal West Pico Chemiluminescent substrate (Pierce). Luminescence was measured in a TopCount machine (Packard Instrument Co., Meriden, CT). The immunoprecipitates captured onto protein A were subjected to Western blotting with densitometry to normalize the levels of tyrosine kinase activity to the receptor protein content in the reactions.

Receptor binding assays. Studies were performed to determine if impaired insulin signaling was associated with reduced ligand binding to the corresponding receptors. Fresh frozen tissue (~100 µg) was homogenized in five volumes of NP-40 lysis buffer (50 mM Tris-HCl, pH 7.5, 1% NP-40, 150 mM NaCl, 1 mM EDTA, 2 mM EGTA) containing protease (1 mM PMSF, 0.1 mM TPCK, 1 µg/ml aprotinin, 1 µg/ml pepstatin A, 0.5 µg/ml leupeptin, 1 mM NaF, 1 mM $Na_4P_2O_7$) and phosphatase (2 mM Na_3VO_4) inhibitors. Protein concentration was determined using the bicinchoninic acid (BCA) assay (Pierce). Exploratory studies were conducted to determine the amounts of protein and concentrations of radiolabeled ligand required to achieve 20% specific binding. Insulin receptor binding assays were performed using 250 µg protein. IGF-I binding assays required 25 µg protein per sample, and IGF-II receptor binding assays were performed with 10 µg protein. Competitive equilibrium binding assays were used to assess growth factor binding levels in relation to ethanol exposure dose. For total binding, duplicate individual protein samples were incubated in 100 µl reactions containing binding buffer (100 mM HEPES, pH 8.0, 118 mM NaCl, 1.2 mM $MgSO_4$, 8.8 mM dextrose, 5 mM KCl, 1% bovine serum albumin) and 100 nCi/ml of ^{125}I-labeled (2000 Ci/mmol; 50 pM) insulin, IGF-I, or IGF-II. To measure nonspecific binding, replicate samples were identically prepared but with the addition of 0.1 µM unlabeled (cold) ligand.

All reactions were performed in 1.5-ml Eppendorf tubes, and the incubations were performed at 4 °C for 16 h with gentle platform agitation. Bound radiolabeled tracer was then precipitated by adding 500 µl 0.15% bovine gamma globulin (prepared in 100 mM Tris-HCl, pH 8.0) followed by 400 µl 37.5% polyethylene glycol 8000 (PEG-8000; prepared in 100 mM Tris-HCl, pH 8.0) to each tube. The samples were thoroughly mixed by vortexing, and then incubated on ice for at least 2 h. The precipitates were collected by centrifuging the samples at 15 000 *g* for 5 min at room temperature. The supernatant fraction, which contained unbound (free) ligand, was transferred in its entirety to a Gamma counting tube (Sarstedt, Newton, NC). Then the tip of the Eppendorf tube with the pellet was cut and released directly into a separate Gamma counting tube. The samples were counted for 1 min each in an LKB CompuGamma CS Gamma counter. Specific binding was calculated by subtracting fmol of nonspecific binding, *i.e.* amount bound in the presence of cold ligand, from the total fmol bound (absence of unlabeled competitive ligand). The results were analyzed and plotted using the GraphPad Prism 4 software (GraphPad Software, Inc., San Diego, CA).

***In vitro* studies using neuronal cultures.** *In vitro* experiments were used to examine the effects of ethanol on receptor binding and ChAT and AChE expression in cerebellar neurons. Primary neuronal cultures were generated with postnatal day 8 rat pup cerebellar tissue [30]. The cultures were maintained with Dulbecco's modified Eagle's medium (DMEM) supplemented with 5% fetal calf serum, 4 mM glutamine, 100 µM nonessential amino acid mixture (Gibco-BRL, Grand Island, NY), 25 mM KCl, and 9 g/L glucose. Ethanol treatment was accomplished by placing the cultures (seeded in 6-well dishes or 96-well plates) in sealed chambers in which 50 mM ethanol was vaporized from a reservoir tray [17, 31]. Control cultures were identically treated but with water added to the reservoir tray. The chambers were flushed with gas containing 75% nitrogen, 20% oxygen, and 5% carbon dioxide. After 96-h incubation at 37 °C, the cells were harvested to measure insulin, IGF-I, and IGF-II receptor binding. Alternatively, the cells were serum-starved for 12 h and then stimulated with 10 nM insulin, 10 nM IGF-I, 25 nM IGF-II, or vehicle for 16 h, and RNA was harvested to measure ChAT and AChE expression. Parallel 96-well cultures stimulated with growth factors for 10 min were used to measure ATP, or for 16 h to measure viability, and ChAT or AChE immunoreactivity. To investigate the role of membrane cholesterol content in relation to receptor binding, control and ethanol-exposed cells were treated with vehicle, 10 mM methyl-β-cyclodextrin (MβCD), or 10 mM aqueous soluble cholesterol in Locke's buffer (154 mM NaCl, 5.6 mM KCl, 2.3 mM $CaCl_2$, 1.0 mM $MgCl_2$, 3.6 mM $NaHCO_3$, 5 mM glucose, 5 mM HEPES, pH 7.4) for 3 h and then harvested for binding assays. To examine the effects of membrane cholesterol content on growth factor stimulated neuronal viability and function, identically treated 96-well cultures were stimulated with vehicle, 10 nM insulin, 10 nM IGF-I, or 25 nM IGF-II for 10 min and then analyzed for ATP content, or for 16 h and then used to measure viability and ChAT or AChE immunoreactivity with the MICE assay [32]. ATP content was measured with the ATPLite assay (Packard). Viability was measured using the CyQuant assay (Molecular Probes, Eugene, OR). Immunoreactivity was measured

directly in the cultured wells using the microtiter immunocytochemical ELISA (MICE) assay [32].

Cholesterol assays. Cholesterol content was measured using the Amplex Red assay kit (Molecular Probes) according to the manufacturer's protocol. Preliminary studies demonstrated that the cholesterol levels and inter-group differences detected in lipid (chloroform: methanol) extracts were comparable to those measured in RIPA buffer extracts, as indicated by the manufacturer. Therefore, it was not necessary to perform the analyses with lipid extracts of the tissue samples. Briefly, tissue homogenates were prepared in RIPA buffer as described above. Samples, serially diluted in 1 × reaction buffer (provided with the kit), were incubated with 150 µM Amplex Red reagent, 1 U/ml horseradish peroxidase, 1 U/ml cholesterol oxidase, and 0.1 U/ml cholesterol esterase in final reaction volumes of 100 µl. Reactions were incubated at 37 °C for 30 min and fluorescence was measured in a Fluorocount microplate reader (Packard) (excitation 560 nm, emission 590 nm). A standard curve was simultaneously generated using a cholesterol standard provided with the kit. The levels of cholesterol were normalized to protein concentration in the samples.

Source of reagents. Human recombinant [^{125}I]insulin, IGF-I, and IGF-II were purchased from Amersham Biosciences. Unlabeled human insulin, recombinant IGF-I, and recombinant IGF-II were obtained from Bachem (Torrance, CA). QuantiTect SYBR Green PCR Mix was obtained from (Qiagen). Antibodies to single-stranded DNA were purchased from Chemicon, and antibodies to ChAT and AChE were obtained from Abcam Inc. (Cambridge, MA). Reagents for immunohistochemical staining were purchased from Vector Laboratories. All other fine chemicals were purchased from either CalBiochem (Carlsbad, CA) or Sigma-Aldrich (St. Louis, MO).

Statistical analysis. Data depicted in the graphs represent the means ± SEM for each group. Inter-group comparisons were made using Student's *t*-tests or analysis of variance (ANOVA) with the Tukey-Kramer *post-hoc* test for significance. Statistical analyses were performed using the Number Cruncher Statistical System (Dr. Jerry L. Hintze, Kaysville, UT) or GraphPad Prism 4 software (GraphPad Software). The computer software generated p values are indicated over the graphs; p values < 0.05 were considered statistically significant.

Results

Dose-effect of chronic gestational exposure to ethanol on birth weight and cerebellar development. Pup birth weights in the 8%, 18%, 26% ethanol groups were not significantly reduced relative to control. However, pups from dams that were fed with the 37% ethanol-containing diet had a significantly lower mean body weight relative to control ($p < 0.05$; Table 2). Although pups in the 8% ethanol diet group had the highest mean body weight relative to control ($p < 0.01$), they nonetheless sustained multiple abnormalities in CNS gene expression and function similar to the other ethanol-exposed groups, suggesting that ethanol-induced neurotoxicity in the developing CNS can occur with normal or increased birth weight. One potential interpretation of the increased birth weight in the low ethanol exposure group is that the pups mainly exhibited effects of insulin resistance, similar to that which occurs in the offspring of Type 2 diabetics. At the highest concentration of ethanol used, the blood alcohol levels achieved (Table 2) were within the range legally regarded as intoxicating in humans, and previously observed in alcoholics taken to an emergency room for acute care [33, 34].

Histopathological studies of H&E-stained cerebella revealed ethanol dose-dependent structural abnormalities related to cell density, cytoarchitecture, and cell migration. Control cerebella had well-delineated foliation (folding) and lamination of the cortex with discrete boundaries corresponding to the external and internal granule cell, Purkinje cell, and molecular layers, and densely populated granule cell layers with only scattered apoptotic (condensed or fragmented) nuclei. With increasing ethanol dose, the cerebellar cortex foliation became progressively simplified, the cortical lamination became less discrete, and the cell density within the granule layers declined (Fig. 1a, d, g, j, m). Reduced cortical foliation was associated with flattening and

Table 2. Effects of chronic gestational exposure to ethanol on birth weight.

Ethanol dose	0%	8% (2%)	18% (4%)	26% (6.5%)	37% (8.2%)
Birth weight (g)	5.2 ± 0.3	6.2 ± 0.5**	4.9 ± 0.5	4.6 ± 0.5	3.9 ± 0.3*
No. of pups	12	13	11	10	8
Blood alcohol level (mM)	0	7.8 ± 2.6*	20.9 ± 5.6**	31.3 ± 8.3**	51.1 ± 11.9**

Pregnant dams were fed with Lieber-DiCarli isocaloric liquid diets containing different concentrations of ethanol as a percentage of the caloric content or (v/v) beginning on gestation day 6 and continuing through pregnancy. Pups were weighed immediately after birth. Maternal blood was obtained after delivery to measure blood alcohol concentration. The data show the mean ± SD of results. Data were analyzed statistically using ANOVA with the Tukey-Kramer *post-hoc* significance test. Significant p values are relative to control (*$p < 0.05$; **$p < 0.005$).

broadening of the cortical surface and limited sulcation (shallow grooves). The reduced delineation of the cortical layers was associated with broadening and irregular lamination of the inner granule and Purkinje cell layers, and narrowing of the external granule cell and molecular layers. Higher magnification images of the external granule cell layer demonstrated progressive ethanol-dose dependent reductions in cell density. In the 37% ethanol group, cell loss and apoptosis were conspicuous, and the residual cell types differed from control in that many of the cells had morphological features of glia (pale vesicular nuclei) rather than neuroblastic elements (compactly arranged small round or oval nuclei with dense chromatin) (Fig. 1b, e, h, k, n). Immunohistochemical staining to detect single-stranded DNA, which corresponds to DNA breakage prior to apoptosis, revealed ethanol dose-dependent increases in the densities of labeled nuclei (Fig. 1c, f, i, l, o). However, the prominent cell loss and apoptosis

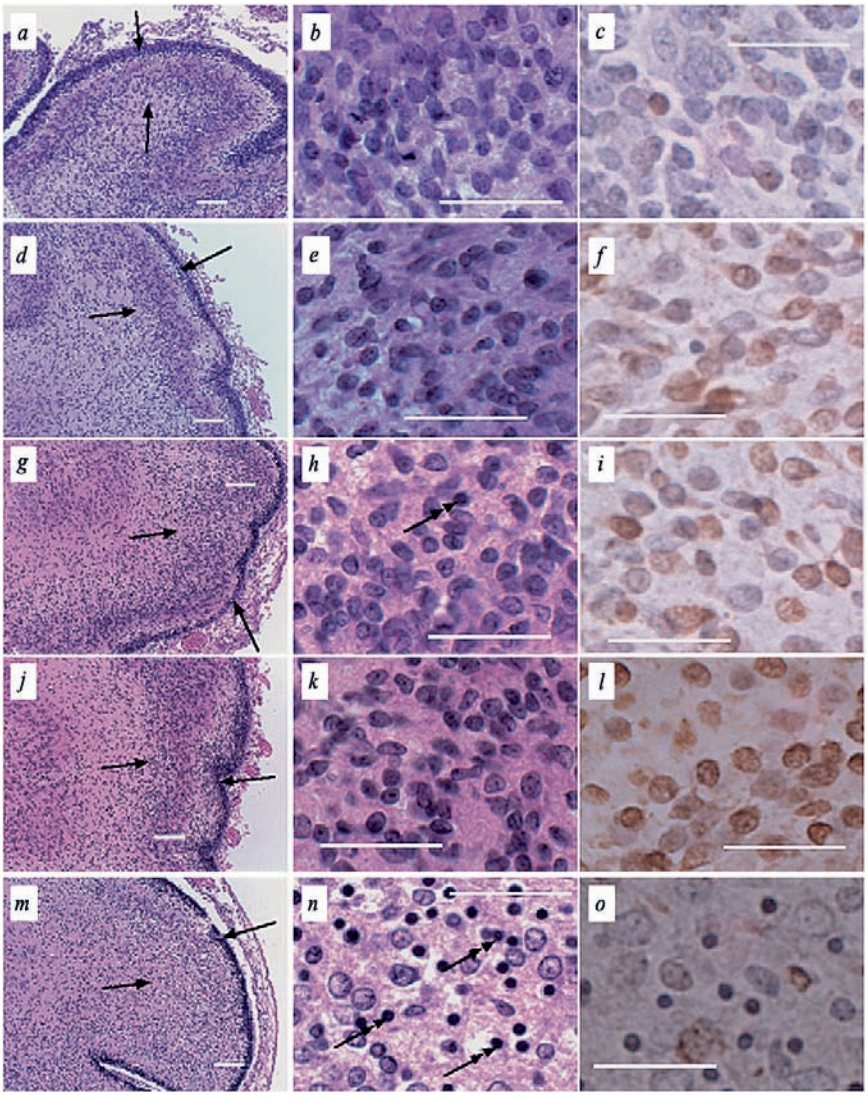

Figure 1. Effects of chronic gestational exposure to different levels of ethanol on cerebellar development. Pregnant dams were fed with Lieber-DiCarli isocaloric liquid diets containing 0% (control; *a–c*), 8% (*d–f*), 18% (*g–i*), 26% (*j–l*), or 37% (*m–o*) ethanol by caloric content, or 0%, 2%, 4.5%, 6.5%, or 9.25% v/v ethanol, beginning on gestation day 6 and continuing through pregnancy. Brains were harvested immediately after birth and immersion fixed in Histochoice fixative. The specimens were embedded in paraffin and histological sections were stained with H&E (*a*, *b*, *d*, *e*, *g*, *h*, *j*, *k*, *m*, *n*). Cerebella from 12 rat pups per group (taken from four or five litters) were used for these studies. Low magnification images were used to demonstrate the effects of ethanol on the structure of the cerebellar cortex including foliation and delineation of the cortical lamination (*a*, *d*, *g*, *j*, *m*; arrows along the top or right side of the image point to the external granule cell layer, whereas the arrows pointing from the left or bottom of the image indicate to the inner zone of the internal granule cell layer; scale bars = 60 μm). Higher magnification images (*b*, *e*, *h*, *k*, *n*; scale bars = 40 μm) illustrate the relative density of cells within the internal granule cell layer. Arrows in *h* and *n* show condensed pyknotic nuclei. To detect DNA damage, adjacent histological sections were immunostained with antibodies to single-stranded (nicked or fragmented) DNA, and immunoreactivity was revealed using the ABC method with DAB (brown) as the chromogen (*c*, *f*, *i*, *l*, *o*). The sections were counterstained lightly with hematoxylin to delineate the tissue architecture. Note the nuclear immunoreactivity for single-stranded DNA (scale bars = 25 μm).

in the 37% ethanol group was associated with relatively reduced nuclear labeling, probably because many cells had already undergone apoptosis.

General comments regarding quantitative RT-PCR studies. The use of real-time quantitative RT-PCR enabled all samples to be analyzed simultaneously and with sufficient replicates to demonstrate consistency of results. With the techniques employed, the quality of the cDNA templates generated from brain tissue was judged to be excellent based on the similar 18S C_t values and consistent 28S:18S ratios obtained for both the control and ethanol-exposed brains. In addition, the 28S:18S ratios were uniformly comparable to the values obtained for RNA isolated from primary neuronal cultures or cell lines. Typically, with cDNA prepared from 10 ng total RNA, the 18S C_t values ranged from 8 to 10, and the calculated 28S/18S ng ratios ranged from 2.0 to 2.2 as previously reported for brain tissue using Northern blot or slot blot analysis [35, 36]. The use of real-time quantitative RT-PCR was ideally suited for rigorous analysis of gene expression in brain tissue because the amplicons were small (mainly < 150 bp), thereby circumventing any potential problems related to partial RNA degradation, *e.g.* nicking, which may increase with oxidative stress or sample processing. The specificity of the amplified products was verified by direct nucleic acid sequencing. Control studies in which cDNA templates were excluded, RNA was not reverse transcribed, the RNA samples were pre-treated with RNase A prior to the RT step, or genomic DNA was used instead in the reactions produced no detectable amplified products by real-time PCR analysis and agarose gel electrophoresis. Treatment of the RNA samples with DNase I prior to the RT step had no effect on the detection levels of amplified gene products.

Ethanol-induced pathological shifts in cell type in the cerebellum. To determine if the ethanol dose-dependent increases in cerebellar hypoplasia and apoptosis produced pathological shifts in the remaining cell populations, real-time quantitative RT-PCR studies were used to measure mRNA transcripts encoding Hu neuronal ribosomal RNA binding protein [37–39], MAG-1 for oligodendroglia, GFAP for astrocytes, AIF-1 for microglia [40, 41], and ET-1 for endothelial cells. The ng quantities of each specific mRNA transcript detected were normalized to the 18S RNA levels measured in the same samples, and results from 8 to 12 animals per group were analyzed statistically. The studies demonstrated ethanol-mediated reductions in Hu and MAG-1 expression, and increases in GFAP and AIF-1 expression, but no significant alteration in ET-1 (Fig. 2). The inhibitory effects on Hu and the stimulatory effects on GFAP and AIF-1 were ethanol dose dependent, whereas the inhibitory effects on MAG-1 expression were similar for all ethanol dosages utilized.

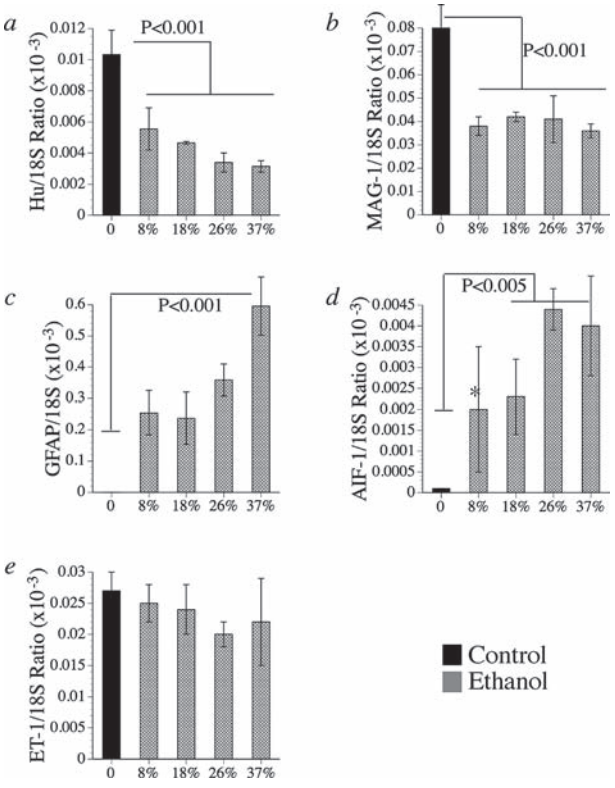

Figure 2. Pathological shifts in cerebellar cell populations following chronic gestational exposure to ethanol. Pregnant dams were fed with isocaloric liquid diets containing 0%, 8%, 18%, 26%, or 37% ethanol by caloric content, or 0%, 2%, 4.5%, 6.5%, or 9.25% v/v ethanol, beginning on gestation day 6 and continuing through pregnancy. RNA extracted from cerebellar tissue (harvested at birth) was used to measure gene expression corresponding to (*a*) neurons (Hu), (*b*) oligodendroglia (MAG-1), (*c*) astrocytes (GFAP), (*d*) microglia (AIF1), and (*e*) endothelial cells (ET-1) by real-time quantitative RT-PCR (see Methods). The values were normalized to 18S rRNA measured in the same samples. Graphs depict the mean ± SEM levels of gene expression in cerebellar tissue from 12 rat pups per group. Inter-group comparisons were made using ANOVA with the *post-hoc* Tukey-Krammer significance test. Significant p values relative to control are indicated above the bars or with an asterisk (*$p < 0.05$).

Effects of ethanol on cerebellar expression of insulin, IGF-I, and IGF-II, and the insulin, IGF-I, and IGF-II receptors. Real-time quantitative RT-PCR studies detected mRNA transcripts corresponding to insulin, IGF-I, and IGF-II polypeptide genes, and insulin, IGF-I, and IGF-II receptors in both control and ethanol-exposed cerebella (Fig. 3). Insulin and IGF-II were more abundantly expressed than IGF-I. Gestational exposure to ethanol produced significant reductions in insulin gene expression that were not dose dependent, *i.e.* even low levels of ethanol exposure inhibited insulin gene expression (Fig. 3a). Gestational exposure to ethanol also caused modest reductions in the levels of IGF-I (Fig. 3c) and IGF-II (Fig. 3e), although the trends were not dose dependent. Insulin and IGF-I receptor mRNA levels were similar, and both were 1.5–2.0-fold higher than IGF-II

receptor expression (Fig. 3b, d, f). Chronic gestational exposure to ethanol did not significantly inhibit insulin, IGF-I, or IGF-II receptor expression, although at the highest concentration used, IGF-II receptor expression was reduced relative to control. Ribosomal 18S (Fig. 3g) and 28S (Fig. 3h) levels measured in the same samples were similarly abundant in all groups. Corresponding with the results obtained by RT-PCR, Western blot analysis demonstrated similar levels of insulin and IGF-I receptor expression in control and ethanol-exposed cerebella.

Ethanol impairs insulin and IGF receptor binding. Effective ligand binding is critical to the signaling cascade, and many of the downstream effects of impaired insulin signaling that have been reported in ethanol-exposed brains, including reduced neuronal survival could be mediated by reduced insulin or IGF-I binding in the CNS. Equilibrium binding assays were performed by incubating cerebellar membrane protein extracts with ^{125}I-labeled insulin, IGF-I, or IGF-II as tracer, in the presence or absence of excess cold ligand. The equilibrium binding studies demonstrated higher levels of specific binding (fmol/mg) to the IGF-I (Fig. 4b) and IGF-II (Fig. 4c) receptors compared with insulin receptors (Fig. 4a). The ethanol-exposed groups all had significantly reduced binding to the insulin (Fig. 4a), IGF-I (Fig. 4b) and IGF-II (Fig. 4c) receptors relative to control. In addition, ethanol exposure impaired insulin and IGF-I receptor binding to greater degrees (~80%) than IGF-II receptor binding (~50%). However, the degrees to which receptor binding was impaired were not ethanol dose dependent.

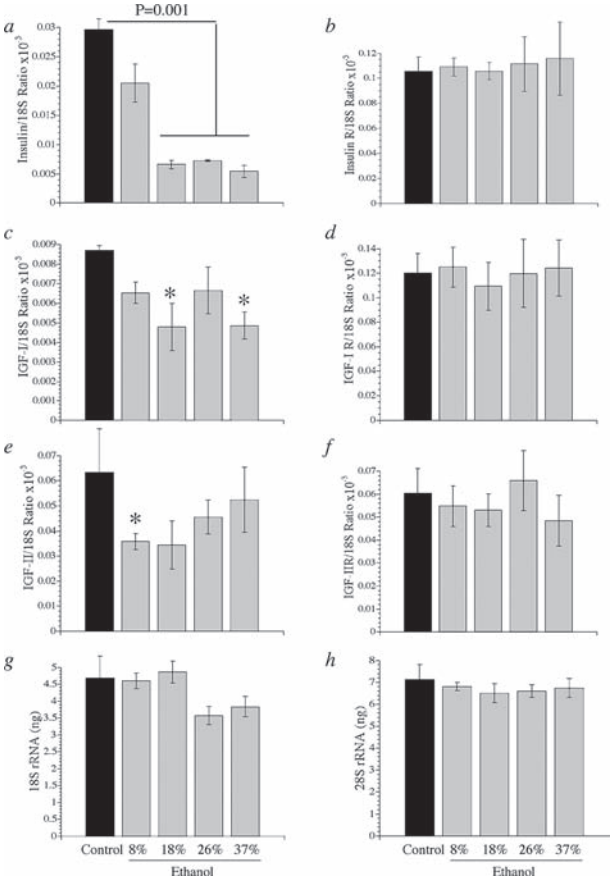

Figure 3. Effects of chronic gestational exposure to different levels of ethanol on cerebellar expression of growth factor and growth factor receptor genes. Pregnant dams were fed with isocaloric liquid diets containing 0%, 8%, 18%, 26%, or 37% ethanol by caloric content from gestation day 6 and through pregnancy. Gene expression corresponding to (*a*) insulin, (*b*) insulin receptor (R), (*c*) IGF-I, (*d*) IGF-IR, (*e*) IGF-II, and (*f*) IGF-IIR mRNA transcripts, and (*g*) 18S and (*h*) 28S ribosomal (r) RNA was measured by real-time quantitative RT-PCR (see methods in legend to Fig. 2) using cerebellar tissue from 9 rat pups per group. Data were analyzed statistically using ANOVA with the Tukey-Kramer *post-hoc* significance test. Significant p values relative to control are indicated above the bars or with an asterisk (*$p < 0.05$).

Effects of gestational exposure to ethanol on insulin and IGF-I receptor tyrosine kinase activities. Studies were done to characterize the degree to which ethanol-associated impairments in receptor binding were associated with reductions in insulin and IGF-I receptor tyrosine kinase activities, and insulin and IGF-I receptor protein expression. Receptor protein levels were measured by Western blotting with digital image densitometry. Receptor tyrosine kinase activities were measured in immunoprecipitates using a non-isotopic luminescence-based assay. The studies demonstrated significantly reduced levels of both insulin- and IGF-I receptor tyrosine kinase activities (Fig. 4d, e), but similar levels of insulin and IGF-I receptor protein expression (Fig. 4f, g) in cerebellar tissue from ethanol-exposed relative to control pups. Corresponding with the binding assay results, the ethanol-associated reductions in receptor tyrosine kinase activity were not dose dependent, and were similarly reduced in cerebella from pups exposed to different *in utero* levels of dietary ethanol. Since the results were normalized to insulin and IGF-I receptor protein levels in the immunoprecipitates (as detected by Western blot analysis with densitometry), the ethanol-associated reductions in insulin and IGF-I receptor tyrosine kinase activities were not attributable to altered growth factor receptor expression. A major consequence of ethanol-impaired insulin and IGF-I signaling in CNS neurons is reduced energy metabolism due to deficiencies in glucose utilization and ATP production [23]. To determine the effects of different levels of chronic *in utero* exposure to ethanol in relation to energy metabolism, ATP content was measured in cerebellar tissue homogenates using a luminescence-based assay. Those studies demonstrated ethanol dose-dependent progressive reductions in cerebellar ATP content, with significant differences from control detected in samples obtained from pups exposed to the 18%, 26%, or 37% ethanol-containing diets (Fig. 4h).

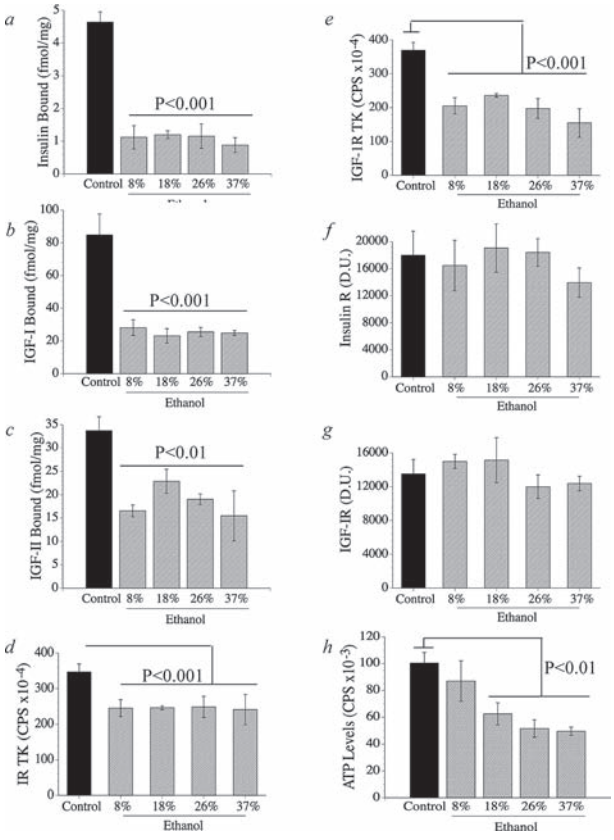

Figure 4. Effects of chronic gestational exposure to different levels of ethanol on competitive equilibrium binding to growth factor receptors, receptor tyrosine kinase activities, receptor protein expression levels, and ATP content in cerebellar tissue. Pregnant dams were fed with isocaloric liquid diets containing 0%, 8%, 18%, 26%, or 37% ethanol by caloric content from gestation day 6 and through pregnancy (see methods in legend to Fig. 2). (*a–c*) To measure ligand binding, cerebellar membrane protein extracts prepared from 10 pups per group were each incubated in duplicate with ^{125}I-labeled insulin, IGF-I, or IGF-II as tracer, in the presence or absence of excess cold ligand. Membrane-bound tracer was precipitated and radioactivity present in the supernatant fractions (unbound) and the pellets (bound) was measured in a gamma counter. Specific binding (fmol/mg) was calculated using the GraphPad Prism 4 software. Graphs depict the mean ± SEM of results obtained for the (*a*) insulin, (*b*) IGF-I, and (*c*) IGF-II specific binding. (*d*, *e*) Insulin or IGF-I receptor immunoprecipitates from 100 µg protein homogenates were analyzed for tyrosine kinase activity using biotinylated synthetic peptide substrates that were captured onto streptavidin-coated surfaces. Tyrosine phosphorylation of the substrates was detected with horseradish peroxidase-conjugated anti-phosphotyrosine and enhanced chemiluminescence reagents. Luminescence counts per second (CPS) were measured in a TopCount machine and normalized to receptor protein levels detected by Western blot analysis of the immunoprecipitates. (*f*, *g*) Insulin (INR) and IGF-I receptor proteins were measured by digital image densitometric analysis of Western blot autoradiographs. The graphs depict the mean ± SEM of results from 10 pups per group. (*h*) ATP levels were measured in homogenates of fresh frozen cerebellar tissue (8 pups per group; 25 µg protein each) using the ATPLite assay. Luminescence (CPS) measured in a TopCount machine was normalized to sample protein content. Data were analyzed statistically using ANOVA with the post-hoc Tukey-Kramer significance test. Significant p values relative to control are indicated over the bar graphs.

Ethanol-associated impairments in acetylcholine homeostasis. Acetylcholine has major functional roles in CNS cognitive and motor systems. Acetylcholine production requires adequate supplies of choline and acetyl-Co-A. Acetyl-Co-A is generated by energy metabolism, which in turn is driven by insulin and IGF-I stimulation. Recent studies demonstrated that ChAT expression is regulated by insulin and IGF-I stimulation [42]. Therefore, it was of interest to determine if ethanol inhibition of insulin and IGF-I signaling mechanisms were associated with deficits in ChAT. Since the steady-state levels of acetylcholine are negatively regulated by AChE, it was also of interest to measure AChE mRNA levels. Real-time quantitative RT-PCR studies demonstrated significant reductions in the mean levels of ChAT (Fig. 5a) and increases in AChE (Fig. 5b) expression in ethanol-exposed cerebellar tissue. The levels of ChAT mRNA were sharply reduced at the lowest ethanol concentration used, and only modest further reductions in ChAT expression with increasing dose of ethanol exposure (Fig. 5a).

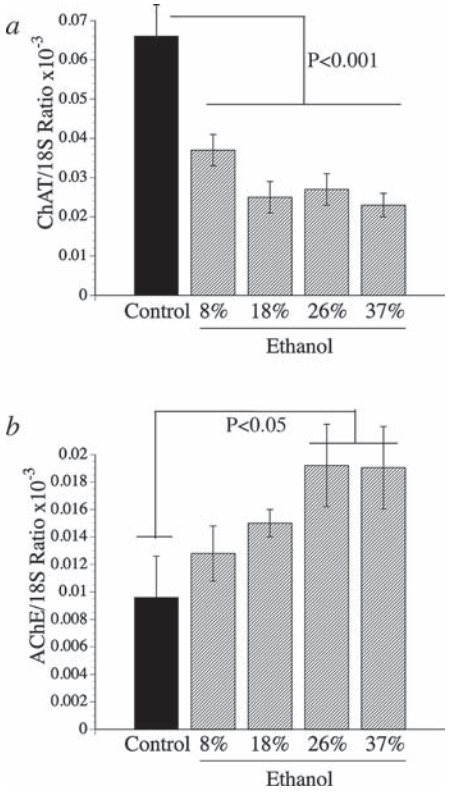

Figure 5. Ethanol-dose effects on cerebellar expression of (*a*) ChAT and (*b*) AChE. Pregnant dams were fed with Lieber-DiCarli isocaloric liquid diets containing 0% (control), 8%, 18%, 26%, or 37% ethanol by caloric content, beginning on gestation day 6 and continuing through pregnancy. Gene expression was measured by real-time quantitative RT-PCR (see methods in Figure 2) using cerebellar tissue from 10 rat pups per group. Data were analyzed statistically using ANOVA with the Tukey-Kramer *post-hoc* significance test. Significant p values relative to control are indicated above the bars.

In contrast, AChE mRNA levels increased progressively with ethanol dose (Fig. 5b).

Short-term *in vitro* ethanol exposure impairs insulin, IGF-I, and IGF-II receptor binding, receptor tyrosine kinase activity, and corresponding growth factor-stimulated ChAT expression. *In vitro* experiments with primary cerebellar neuron cultures were used to help validate the *in vivo* observations, and characterize potential mechanisms by which ethanol causes insulin/IGF resistance. Previous studies demonstrated reduced levels of insulin- and IGF-I-stimulated receptor tyrosine kinase activity in ethanol exposed cerebellar neuron cultures [23]. To determine if this effect of ethanol is mediated by impaired ligand-receptor binding, equilibrium binding assays were performed with membrane proteins harvested from primary rat cerebellar control or ethanol-exposed (50 mM for 96 h) neuronal cultures. The concentration of ethanol used was within the range detected in human alcoholics [33, 34]. ChAT and AChE immunoreactivity were measured directly in the cultured cells using the MICE assay (cellular ELISA), with values normalized to cell density. The results demonstrated significantly reduced levels of insulin (Fig. 6a), IGF-I (Fig. 6b), and IGF-II (Fig. 6c) receptor binding. In addition, the ethanol-treated neuronal cells had significantly reduced basal and insulin-, IGF-I-, or IGF-II-stimulated levels of ATP (Fig. 6d), and basal, insulin-stimulated, and IGF-I-stimulated ChAT immunoreactivity relative to the control (Fig. 6e). AChE immunoreactivity was not prominently modulated by growth factor stimulation, although AChE expression was higher in IGF-II-stimulated compared with corresponding un-stimulated control cells, and in un-stimulated ethanol-exposed relative to un-stimulated control cells (Fig. 6f).

Potential mechanism of impaired insulin and IGF receptor binding and stimulation of ChAT. Membrane cholesterol content can influence ligand binding to cell surface receptors. For example, decreased or increased cholesterol content in membranes has been associated with altered or impaired growth factor binding and signal transduction [43–46]. To determine if the observed differences in receptor binding were correlated with membrane cholesterol content, cholesterol levels were measured in cerebellar membrane extracts. Analysis of the pups' brains (n = 8 per group) demonstrated significantly reduced cholesterol content in ethanol-exposed relative to control cerebellar membranes (Fig. 7a). Cerebellar membrane cholesterol content was reduced by ~50% relative to control in the 8% ethanol diet group, but with higher doses of ethanol, only slight further reductions in membrane cholesterol were observed (Fig. 7a). Similarly, *in vitro* exposure to 50 mM ethanol for 96 h significantly reduced cerebellar neuron membrane cholesterol content (Fig. 7b).

To further explore the role of cholesterol or lipid depletion as a mediator of impaired binding, control and ethanol-exposed (50 mM for 96 h) cerebellar neuron cultures were treated for 3 h with vehicle, 10 mM MβCD, or 10 mM cholesterol in Locke's buffer. The cells were then analyzed for insulin, IGF-I, and IGF-II receptor equilibrium binding. Initial studies demonstrated that treatment with MβCD significantly reduced membrane cholesterol

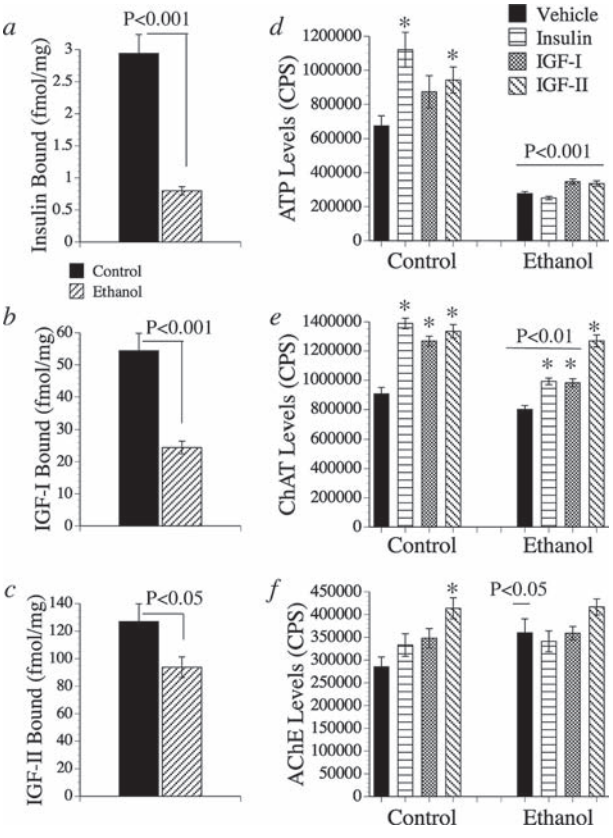

Figure 6. Effects of short-term *in vitro* ethanol exposure on (*a*) insulin, (*b*) IGF-I, and (*c*) IGF-II receptor binding and insulin-, IGF-I-, and IGF-II-stimulated levels of (*d*) ATP, (*e*) ChAT, and (*f*) AChE. Post-mitotic rat primary cerebellar neuron cultures were exposed to vaporized 50 mM ethanol or humidified air in sealed chambers for 96 h, after which the cells were harvested to measure receptor binding in membrane extracts. Equilibrium binding assays were performed as described in the legend to Fig. 4. Graphs depict the mean ± SEM of fmol/mg of specifically bound ligand. Data were analyzed statistically using the Student's *t*-test. Significant p values are indicated over the bar graphs. To measure responsiveness to growth factor stimulation, control and ethanol-treated cells were serum-starved for 16 h, and then stimulated with vehicle, 10 nM insulin, 10 nM IGF-I, or 25 nM IGF-II for 24 h. The cells were analyzed for (*d*) ATP content using the ATPLite assay, and (*e*) ChAT or (*f*) AChE immunoreactivity using the MICE assay with luminescence detection (see Methods). Data (CPS) generated from 16 micro-cultures were averaged and representative results are depicted graphically (mean ± SEM). Results were analyzed statistically using ANOVA with the Tukey-Kramer *post-hoc* significance test. Significant p values relative to the corresponding cultures in the control group are indicated over the bars, and significant differences relative to the same group un-stimulated controls are indicated by the asterisks (*p < 0.05 or better).

content, whereas treatment with cholesterol significantly increased the membrane cholesterol content in both control and ethanol-exposed cerebellar cultures (Fig. 7c). In control and ethanol-exposed cultures, MβCD treatment significantly inhibited insulin (Fig. 7d), IGF-I (Fig. 7e), and IGF-II (Fig. 7f) receptor binding relative to the corresponding vehicle-treated cells, whereas cholesterol treatment enhanced insulin receptor binding in the ethanol-treated cells, but had no significant effect on insulin receptor binding in control cells (Fig. 7d). However, cholesterol treatment significantly impaired IGF-I and IGF-II receptor binding in control cerebellar neurons (Fig. 7e, f). In vehicle-treated ethanol-exposed cells, insulin, IGF-I, and IGF-II receptor binding were significantly reduced relative to the vehicle-treated control cells (Fig. 7d–f), as illustrated in Figure 6. In addition, MβCD treatment of ethanol-exposed cells further reduced insulin receptor binding to levels, which were also significantly reduced relative to the MβCD-treated control cell (Fig. 7d). In contrast, MβCD or cholesterol treatment caused similar degrees of impaired IGF-I and IGF-II receptor binding in control and ethanol-exposed neuronal cells (Fig. 7e, f).

The effects of cholesterol or MβCD treatment on neuronal viability (Fig. 8a–c), ATP production (energy metabolism; Fig. 8d–f), ChAT (Fig. 8g–i) and AChE (Fig. 8j–l) immunoreactivity were examined in cells that were treated as described above and stimulated 12 h with vehicle (control), 10 nM insulin, 10 nM IGF-I, or 25 nM IGF-II in serum-free medium. All assays were performed using 96-well cultures. Viability was measured using the CyQuant assay and ATP content was measured using the ATPLite assay. ChAT and AChE immunoreactivities were measured using the MICE assay [32], which was modified through the use of luminescence detection reagents [19, 27]. In vehicle-treated cells, neuronal viability was significantly reduced in insulin-stimulated, but not in IGF-I- or IGF-II-stimulated ethanol-exposed cultures (Fig. 8a). However, ATP content was significantly reduced in all ethanol-treated cultures, irrespective of growth factor stimulation (Fig. 8d). MβCD or cholesterol treatment broadly reduced neuronal viability and mitochondrial function in both control and ethanol-exposed cultures, but growth factor-stimulated viability and energy metabolism were further reduced in MβCD-treated ethanol-exposed relative to corresponding control cultures (Fig. 8b, c, e, f). In vehicle-treated control cells, ChAT expression was significantly increased by insulin stimulation, whereas in ethanol-exposed cells, ChAT was not modulated by insulin stimulation, and both basal and growth factor-stimulated levels of ChAT were significantly lower than control (Fig. 8g). MβCD treatment of control cells abolished the insulin-stimulated increases in ChAT, but significantly increased IGF-I- and IGF-II-stimulated ChAT (Fig. 8h). In ethanol-exposed cells, MβCD treatment was associated with broadly reduced levels of ChAT expression relative to control, independent of growth factor stimulation (Fig. 8h). In control cells, cholesterol treatment muted basal and growth factor-stimulated ChAT expression, whereas in the ethanol-exposed cells, cholesterol treatment significantly increased the insulin-, IGF-I-, and IGF-II-stimulated levels of ChAT relative to corresponding vehicle-treated cells, resulting in ChAT expression levels that were similar to or higher than control

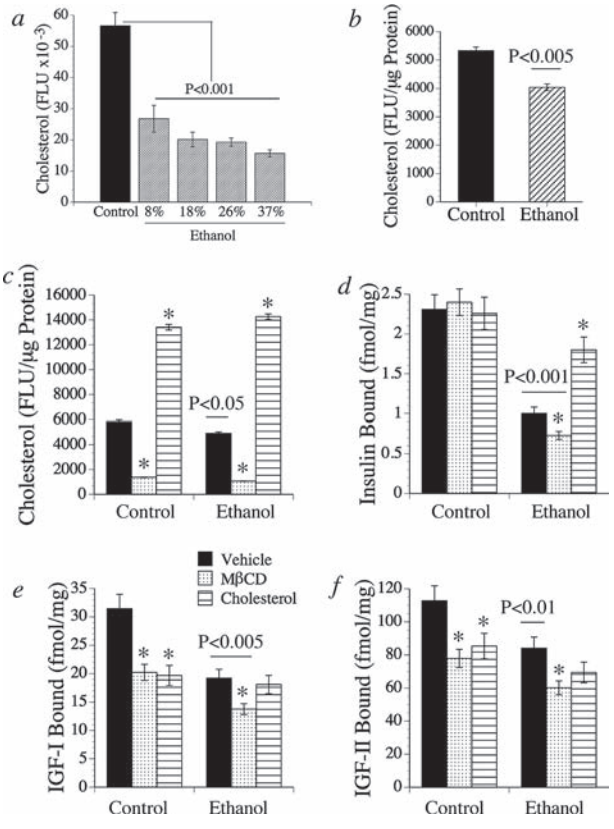

Figure 7. Potential role of decreased membrane cholesterol content in relation to impaired insulin and IGF receptor binding and signal transduction following ethanol exposure. The chronic gestation ethanol exposure model was generated as described in Figure 2. For the *in vitro* ethanol-exposure model, primary post-mitotic rat cerebellar neuron cultures were exposed to vaporized ethanol (50 mM) or air in sealed humidified chambers for 96 h. Cholesterol content was measured in the protein extracts of (*a*) control and ethanol-exposed rat pup cerebellar membranes (n = 8 pups per group), and (*b*) cerebellar neuron cultures using the Amplex Red Cholesterol assay kit and a Fluorocount microplate reader (see Methods). To determine the effects of cholesterol depletion or repletion on growth factor binding, control and ethanol-exposed cerebellar neuron cultures were incubated with vehicle, 10 mM MβCD, or 10 mM cholesterol in Locke's buffer for 3 h at 37 °C. The cells were analyzed for (*c*) membrane cholesterol content and equilibrium binding (fmol/mg protein) to the (*d*) insulin, (*e*) IGF-I, or (*f*) IGF-II receptors as described in Figure 4. The graphs depict the mean ± SEM of results. Data were analyzed using ANOVA with the *post-hoc* Tukey-Kramer significance test. Significant p values relative to vehicle-treated controls (within group) are indicated by asterisks (*$p < 0.05$ or better). Significant between-group (control *versus* corresponding ethanol-treated) differences are indicated by the horizontal lines over the bars.

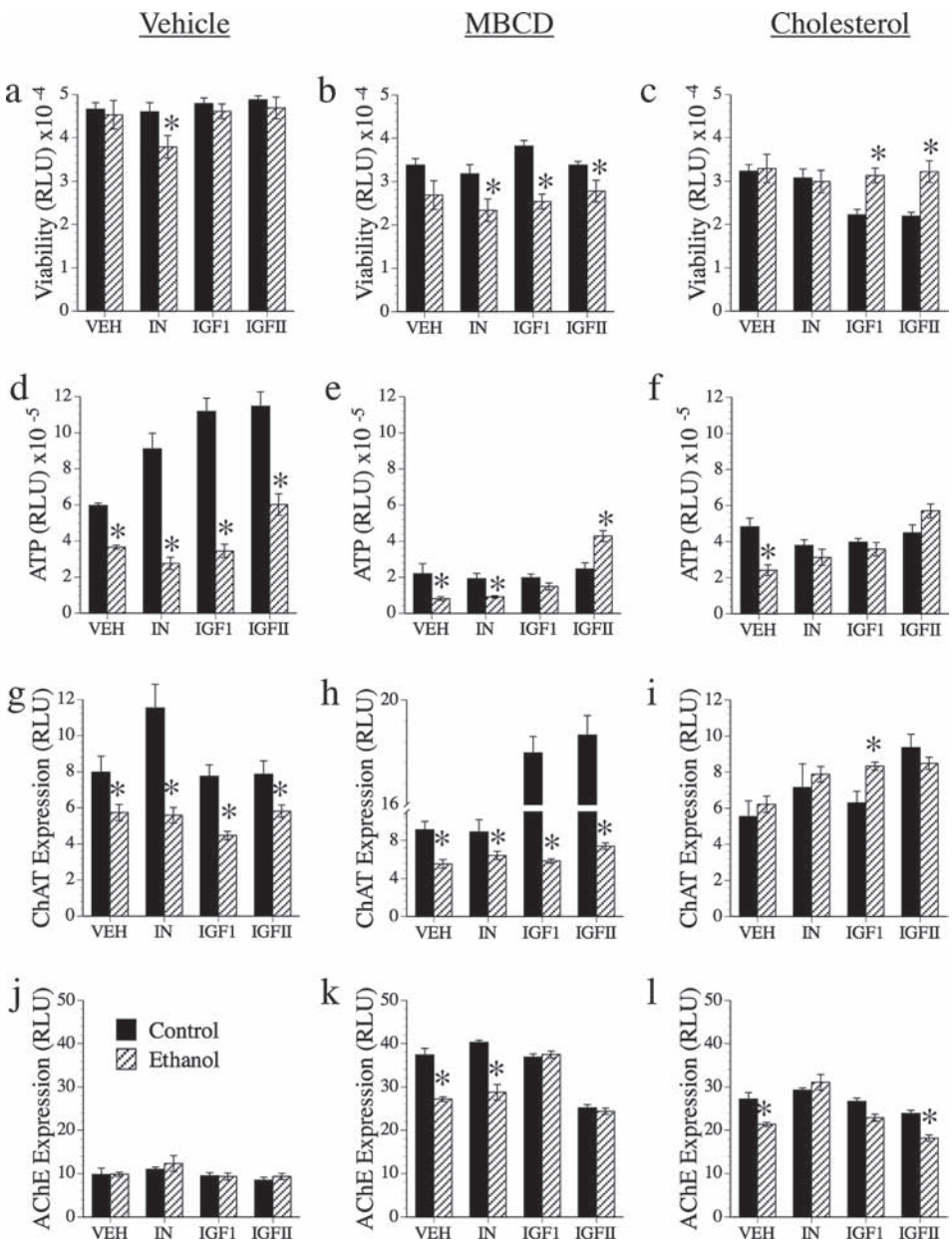

Figure 8. The effects of MβCD or cholesterol treatment on basal and insulin-, IGF-I-, or IGF-II-stimulated neuronal (*a–c*) viability, (*d–f*) ATP content, (*g–i*) ChAT and (*j–l*) AChE expression in control and ethanol-exposed (50 mM for 96 h) primary cerebellar neuron cultures seeded into 96-well plates. Control and ethanol-exposed cells were treated with (*a*, *d*, *g*, *j*) vehicle, (*b*, *e*, *h*, *k*) 10 mM MβCD, or (*c*, *f*, *i*, *l*) 10 mM cholesterol in Locke's buffer for 3 h at 37 °C, and then stimulated with vehicle (VEH), 10 nM insulin (IN), 10 nM IGF-I, or 25 nM IGF-II in serum-free medium for 12 h. Viability was measured using the CyQuant assay. ATP was measured using the ATPLite assay. ChAT and AChE immunoreactivity were measured with the MICE assay with luminescence detection. Replicate cultures ($n = 24$) were analyzed for each assay. The graphs depict the mean ± SEM of results. Data were analyzed using ANOVA with the *post-hoc* Tukey-Kramer significance test. *$p < 0.05$ or better for comparisons between control and ethanol-exposed cells for each condition. +$p < 0.05$ or better for within-group comparisons to the corresponding vehicle-treated cells.

(Fig. 8i). In effect, cholesterol treatment rescued the ethanol-exposed cells by restoring ChAT expression to control levels in the presence of growth factor stimulation. However, insulin-stimulated ChAT expression in cholesterol-treated, ethanol-exposed cells was still significantly lower than the insulin-stimulated, vehicle-treated control cells ($p < 0.005$), indicating that the cholesterol rescue was only partial. AChE expression was similar in vehicle-treated control and ethanol-exposed neuronal cells, independent of growth factor stimulation (Fig. 8j). Treatment with MβCD or cholesterol significantly increased the mean levels of AChE in both control and ethanol-exposed cells, with generally greater effects noted for MβCD than cholesterol (Fig. 8k, l). The only notable inter-group dif-

ferences were that the AChE levels were significantly lower in ethanol-exposed relative to control MβCD- or cholesterol-treated+un-stimulated, MβCD-treated + insulin-stimulated, and cholesterol-treated + IGF-II-stimulated cultures (Fig. 8k, l).

Discussion

Graded ethanol effects on cerebellar development. In humans, chronic *in utero* exposure to high levels of ethanol impairs body and brain growth, resulting in small for gestational age infants and increased incidences of microencephaly, reduced white matter volume, ventriculomegaly, and attention deficit hyperactivity disorders [47]. In addition, major structural and functional abnormalities in the basal ganglia and cerebellum account for the prominent motor system deficits associated with human cases of FAS and fetal alcohol spectrum disorders [47]. The FAS-induced cerebellar abnormalities are associated with impairments in neuronogenesis, neuronal survival, neuronal adhesion, and neuronal migration [47–49]. In our experimental model of FAS, chronic gestational exposure to relatively high levels of ethanol (37% caloric content or 9.25% v/v) that resulted in maternal blood ethanol concentrations of 51.1 ± 11.9 mM, significantly reduced the mean birth weight and produced striking teratogenic effects on CNS development in the offspring as previously reported [27]. The analysis of pups with different levels of *in utero* ethanol exposure provided new information about the degree to which ethanol-induced CNS abnormalities could be produced with different ethanol doses. The investigations were focused on the cerebellum because it represents a major CNS target of ethanol neurotoxicity in both humans and experimental animals.

The results from the *in vivo* studies demonstrated mixed responses to the graded doses of ethanol exposure. Dose-dependent adverse effects of ethanol were observed with respect to cerebellar development, neuronal gene expression (neuronal survival), astrocyte and microglial cell proliferation, ATP content (energy metabolism), and ChAT and AChE expression. In contrast, the levels of myelin-associated glycoprotein gene expression, insulin, IGF-I, and IGF-II receptor binding, and insulin and IGF-I receptor tyrosine kinase activities were similarly reduced following exposure to low or high concentrations of dietary ethanol, *i.e.* these adverse effects of ethanol were not graded. Therefore, only some consequences of chronic gestational exposure to ethanol appear to be dose dependent, and may be linked to impaired neuronal survival and attendant proliferation of astrocytes and activation of microglial cells in response to injury. On the other hand, the ethanol dose-independent abnormalities, such as the impairments in receptor binding, may be mediated by other factors such as secondary toxic effects of ethanol and/or its metabolites, but further studies will be required to fully characterize the mechanisms of these responses.

The cerebella of ethanol-exposed pups exhibited hypoplasia, reduced cell survival, and impaired neuronal migration, and the severity of these lesions was graded with respect to ethanol dose. Histopathological studies showed that chronic *in utero* exposure to ethanol produced dose-dependent cell loss associated with increased DNA damage, and marked alterations in the structure (foliation) and cytoarchitecture (lamination) of the cerebellar cortex due to impaired neuronal migration. The molecular studies designed to assess the relative abundance of different brain cell populations demonstrated significantly reduced Hu and MAG-1 expression, corresponding to neurons and oligodendroglia, and increased GFAP and AIF-1, corresponding to astrocytes and microglia, respectively. These results suggest that both neurons and oligodendroglia represent targets of ethanol neurotoxicity in the CNS, and corroborate the previous findings of neuronal loss and reduced white matter volume in human cases of FAS [1–3, 25, 50, 51]. Although the mechanisms of neuronal and oligodendroglial cell loss in the context of chronic gestational exposure to ethanol are not entirely understood, potential mediators include: (1) impairments in insulin-stimulated cell survival due to insulin receptor resistance (see below) and impaired signaling downstream through phosphatidylinositol (PI) 3-kinase [27, 52]; (2) reduced local CNS production of insulin, which is needed for cell survival, *i.e.* trophic factor withdrawal; and (3) increased oxidative stress due to mitochondrial dysfunction [16, 23]. The molecular cell profiling studies also demonstrated increased GFAP expression, which could reflect increased numbers and/or activation of astrocytes following neuronal and oligodendroglial cell loss. In addition, the increased levels of AIF-I could be important with regard to mechanisms of tissue injury since microglia release of cytokines and nitric oxide, leading to increased oxidative stress and mitochondrial dysfunction, which are known mediators of ethanol-induced cell loss both *in vivo* and *in vitro* [16, 19, 20, 27].

Effects of ethanol on cerebellar expression of genes required for insulin and IGF signaling. The cell loss associated with chronic gestational exposure to ethanol selectively reduced the relative populations of neurons and oligodendroglia. Previous studies demonstrated that these cell types are responsive to insulin and/or IGF-1 stimulation, and that intact insulin or IGF-1 signaling mechanisms mediate neuronal and oligodendroglial cell survival [19, 27, 53–58]. Growth factor signaling can be modulated by altering the availability of growth factors, the expression of growth factor receptors, or the responsiveness of receptors to growth factor stimulation. Therefore, it was of interest to determine if the preferential loss of neurons and oligodendroglia in ethanol-exposed cer-

ebella was associated with reduced expression of insulin, IGF-I, IGF-II, or their corresponding receptors.

Real-time quantitative RT-PCR studies demonstrated significant ethanol-associated reductions in the levels of insulin, IGF-I, and IGF-II gene expression, although only the insulin gene expression levels were sharply and consistently reduced at higher levels of ethanol exposure. In contrast, insulin, IGF-I, and IGF-II receptor expression were not consistently affected by in utero exposure to ethanol. Variability in the effects of ethanol on insulin and IGF receptor expression was noted both in the present study, and with respect to previously published results [23]. The explanation for this phenomenon is not obvious, but it suggests that *in vivo*, the genes regulating the expression of insulin and IGF receptors are less vulnerable to the adverse effects of ethanol than are the signaling functions of the corresponding proteins. This concept is supported by the profound inhibitory effect of ethanol on insulin and IGF receptor gene expression detected after chronic *in vitro* ethanol exposure of cultured cerebellar neurons [23]. These results suggest that one mechanism by which ethanol impairs CNS functions that require insulin and IGF signaling is to inhibit local CNS growth factor production. This effect could be mediated by either selective cell killing, or down-regulation of growth factor genes. However, one discordant finding was that insulin and IGF-I receptor tyrosine kinase activities were significantly reduced by gestational exposure to ethanol, irrespective of dose. Moreover, previous *in vitro* studies demonstrated that ethanol impairs insulin and IGF-I receptor tyrosine phosphorylation and kinase activation, despite exogenous supply of the growth factors [16, 18, 27, 59, 60]. These observations suggest that factors other than growth factor gene expression contribute to ethanol-mediated impairment of insulin and IGF signaling in the CNS.

Ethanol-impairs insulin and IGF receptor binding. Effective ligand binding is critical to the signaling cascade, and many of the previously reported downstream adverse effects of ethanol on insulin signaling including reduced neuronal survival could be mediated by impaired insulin or IGF-I binding in the CNS. The equilibrium binding assays demonstrated higher levels of specific binding to the IGF-I and IGF-II receptors relative to the insulin receptor in control brains, and reduced binding to the insulin, IGF-I and IGF-II receptors in ethanol-exposed relative to control brains. In addition, chronic gestational ethanol exposure impaired binding to the insulin and IGF-I receptors to greater extents (~80%) than to the IGF-II receptors (~50%). However, the inhibitory effects of ethanol on insulin, IGF-I and IGF-II binding were not dose dependent, and instead the degree to which binding was reduced was similar among the different ethanol-dosage groups. Therefore, despite relatively preserved levels of insulin and IGF receptor expression, ligand binding to the receptors was markedly reduced following chronic *in utero* exposure to ethanol. Further *in vitro* studies showed that ligand binding was also impaired after relatively brief periods (96 h) of ethanol exposure. These results suggest that the inhibitory effects of ethanol on insulin and IGF signaling required for cell survival and energy metabolism in the brain are mediated at the level of receptor binding, *i.e.* the most proximal point in the signal transduction cascade.

The potential consequences of impaired signaling through the insulin and IGF-I receptors include reduced signaling downstream through insulin receptor substrate (IRS) molecules and decreased activation of pathways required for cell growth and survival. However, the effects of impaired IGF-II gene and receptor expression are less well understood. IGF-II is expressed in various regions of the fetal brain [61, 62], but mainly in cells of mesenchymal and neural crest origin [61]. IGF-II receptors are also widely distributed in fetal brains [61, 62]. Targeted gene mutation studies demonstrated that IGF-II stimulates prenatal brain growth and activates insulin-stimulated signaling pathways via the insulin receptor [63]. Although IGF-II receptors may also function as scavengers for IGF-II by promoting transport and degradation of the protein [64], there is growing evidence that IGF-II can stimulate growth and motility through activation of its own receptor [65, 66]. In this regard, IGF-II-stimulated growth and motility signals can be transmitted through G-coupled proteins via IRS-independent pathways [67]. In addition, cellular proliferation in response to IGF-II stimulation can be mediated by signaling through the insulin and IGF-I receptors, thereby converging to IRS pathways.

Chronic gestational exposure to ethanol impairs insulin and IGF-I receptor tyrosine kinase activation. Previous studies demonstrated ethanol inhibition of insulin receptor tyrosine phosphorylation and kinase activity, compared with intact insulin receptor protein expression [23, 27]. We extended this line of investigation by characterizing ethanol-dose effects on insulin and IGF-I receptor tyrosine kinase activities. The results demonstrated that chronic gestational exposure was associated with significantly reduced levels of insulin and IGF-I receptor tyrosine kinase activities; however, corresponding with the non-tiered effects of ethanol on ligand binding, the ethanol-associated reductions in insulin and IGF-I receptor tyrosine kinase activities were also not graded, and instead the levels were similarly reduced in all ethanol-exposed groups relative to control. This suggests that at least some aspects of insulin and IGF-I signaling in the brain are substantially impaired by relatively low levels of chronic gestational exposure to ethanol. To determine if these adverse effects of ethanol required long-term exposure, *in vitro* experiments were conducted using cerebellar

neuron cultures that were treated with 50 mM ethanol for 4 days. The findings of reduced insulin and IGF binding, and the previously observed reductions in insulin- and IGF-I-stimulated tyrosine kinase activation [23] in the ethanol-treated neuronal cultures indicate that short-term ethanol exposure, such as with binge drinking, can also have pronounced inhibitory effects on insulin and IGF-I receptor function. The proximal nature of this molecular lesion provides a means by which ethanol could interfere with diverse downstream functions that are mediated by insulin or IGF-I signaling, including cell survival and energy metabolism.

Consequences of ethanol impaired insulin and IGF-I signaling in relation to brain function. Since ChAT expression is regulated by insulin and IGF-I stimulation [42], and acetylcholine is a major neurotransmitter that mediates CNS cognitive and motor functions, it was of interest to determine if the inhibitory effects of ethanol on insulin and IGF-I signaling in the brain impaired acetylcholine homeostasis. The real-time quantitative RT-PCR studies demonstrated reduced levels of ChAT and increased levels of AChE gene expression in ethanol-exposed cerebella. In addition, *in vitro* studies demonstrated that basal, insulin-stimulated, and IGF-I-stimulated levels of ChAT immunoreactivity were significantly reduced in cerebellar neuron cultures after 4 days of ethanol exposure, at a time when the cultures were post-mitotic and significant cell loss was not detected. Potential mechanisms by which ethanol exposure leads to reduced ChAT expression include, inhibition of insulin/IGF-I signaling and, with chronic *in vivo* exposure, impaired survival of ChAT-expressing neurons. The increased AChE expression observed after chronic *in utero* exposure to ethanol could be explained on the basis astrocytic and microglial cell proliferation and/or activation following death of neurons and oligodendroglia.

Ethanol impaired insulin and IGF receptor binding are linked to altered membrane lipid composition. Cerebella from rat pups that were chronically exposed to ethanol *in utero* were found to have significantly reduced levels of membrane cholesterol relative to control cerebella. In addition, membrane cholesterol content was significantly reduced in cerebellar neuron cultures that were subjected to short-term ethanol exposure, indicating that even short-term ethanol exposure can alter the lipid composition of brain cell membranes. *In vitro* experiments demonstrated that MβCD depletion of membrane cholesterol, significantly inhibited IGF-I and IGF-II binding in control cells and insulin, IGF-I and IGF-II binding in ethanol-exposed cells. Cholesterol treatment, which resulted in increased cholesterol content in cerebellar neuron membranes, also inhibited IGF-I and IGF-II receptor binding in control and ethanol-exposed cells. These findings are consistent with the concept that cholesterol influences ligand-receptor interactions by altering the membrane fluidity or the inter-molecular interactions [68]. However, cholesterol treatment did not impair insulin receptor binding in control cells, and it significantly increased insulin receptor binding in ethanol-exposed cells. The fact that the rescue was incomplete suggests that other lipids depleted by ethanol exposure are also important for mediating insulin receptor binding. These results are consistent with a previous report demonstrating that cholesterol and lipid content and composition in membranes can significantly influence ligand binding to cell surface receptors and attendant downstream intracellular signaling [45]. The relative preservation of insulin receptor binding in MβCD-treated control cells, and incomplete rescue of insulin receptor binding produced by cholesterol treatment of ethanol-exposed cells suggest that other lipids present in caveolae, that are not depleted by MβCD but are reduced by ethanol treatment, may be critical mediators of insulin receptor binding.

Role of membrane cholesterol content in insulin and IGF-I signaling. Previous studies demonstrated that MβCD treatment, which depletes membrane cholesterol, causes insulin resistance [69, 70], and that cholesterol addition, which effectively alters membrane lipid composition in otherwise normal cells, also decreases insulin responsiveness [45]. In neuronal cells, tyrosine kinase receptors are distributed in the low-density membrane fraction corresponding to caveolae [71], and in general, insulin receptors signal within caveolae microdomains. Experimentally, MβCD chelation of cholesterol and attendant disruption of caveolae inhibits insulin receptor tyrosine kinase auto-activation, and insulin-stimulated glucose uptake [72, 73]. Further investigations localized a portion of the IRS-I molecule to caveolae and showed that treatment with relatively low concentrations of MβCD (2 mM), which does not inhibit insulin receptor auto-phosphorylation or IRS-I tyrosine phosphorylation, disrupts caveolae/lipid rafts and the downstream insulin and IRS-I signaling mechanisms [74, 75], with reduced activation of the IRS-1-PI3 kinase-Akt pathway [76], and in some instances, preservation of MAPK signaling [70]. Therefore, apart from its inhibitory effects on receptor binding, cholesterol depletion may impair insulin signaling downstream of its receptor through PI3 kinase due to disruption of caveolae microdomains.

In previous studies, we demonstrated that ethanol exposure also selectively impairs insulin- and IGF-I-stimulated PI3 kinase-Akt in immature neurons and the developing brain [16, 19, 23, 27, 52], suggesting that some of the adverse effects of ethanol on survival signaling and mitochondrial function are mediated through pathological alterations in the cholesterol and lipid composition of caveolae and lipid rafts. However, it is noteworthy that

the properties of insulin signaling in relation to its dependence on caveolar integrity can vary with tissue and cell type. For example, in the liver, caveolar gene depletion does not inhibit insulin receptor activation and signaling because ligand-bound receptors can be recruited to lipid rafts to mediate signaling [77]. Although IGF-I signaling through IRS-I-Akt is also impaired by cholesterol depletion [44, 78], IGF-I signaling was localized to lipid rafts and shown to be caveolae independent [79]. The distinct subcellular localizations of insulin and IGF-I signaling in caveolae *versus* lipid rafts could partially account for the differential effects of insulin and IGF-I stimulation, despite highly overlapping downstream pathways.

Effects of ethanol and cholesterol depletion/repletion on insulin-, IGF-I-, and IGF-II-stimulated acetylcholine homeostasis mechanisms. The finding that ChAT expression was markedly increased in MβCD-treated IGF-I- or IGF-II-stimulated control cells, despite significantly reduced binding relative to corresponding vehicle-treated cells provides further evidence that insulin- and IGF-stimulated functions are not strictly related to binding. Similarly, in ethanol-exposed cells, cholesterol treatment significantly enhanced only insulin receptor binding, yet insulin-, IGF-I-, and IGF-II-stimulated ChAT were all significantly increased relative to corresponding vehicle-treated cells. Therefore, insulin- and IGF-stimulated ChAT expression are prominently regulated by membrane cholesterol content and lipid composition. In control cells, reducing cholesterol content dramatically increased IGF-I- and IGF-II-stimulated ChAT, whereas increased cholesterol blunted the insulin-stimulated increase in ChAT. This suggests that in control cells, reduced cholesterol relative to other membrane lipids may enhance acetylcholine biosynthesis through lipid raft but not caveolar-dependent (insulin) signaling mechanisms. In contrast, cholesterol treatment rescued ethanol-exposed neuronal cells by enhancing insulin-, IGF-I- and IGF-II-stimulated ChAT expression. Therefore, membrane lipid and cholesterol content have critical roles in modulating neuronal responses to insulin- and IGF-stimulated ChAT expression and acetylcholine biosynthesis. The finding of broadly increased levels of AChE expression in MβCD- or cholesterol-treated control and ethanol-exposed cells were unexpected. However, one potential explanation for this result is that substantial increases or decreases in membrane lipid composition may impair growth factor-stimulated energy metabolism. This interpretation is consistent with our finding that either MβCD or cholesterol treatment reduced energy metabolism and viability in neuronal cells, independent of growth factor stimulation (Fig. 8). Impaired energy metabolism could cause oxidative stress, and recent studies demonstrated that oxidative stress increases AChE function [80, 81]. The results linking ethanol-impaired insulin and IGF-I signaling to reduced levels of ChAT and increased levels of AChE, *i.e.* perturbations in acetylcholine homeostasis, as well as mediators of neuro-inflammation and oxidative stress (impaired energy metabolism, increased microglia and astrocytes) in the brain, suggest important and novel mechanisms by which chronic gestational exposure to ethanol leads to developmental deficits in CNS cognitive and motor functions.

Acknowledgements. Supported by Grants AA02666, AA-02169, AA-11431, AA12908, and COBRE P20RR15578 from the National Institutes of Health.

1 Clarren, S. K., Alvord, E. J., Sumi, S. M., Streissguth, A. P. and Smith, D. W. (1978) Brain malformations related to prenatal exposure to ethanol. J. Pediatr. 92, 64–67.
2 Mattson, S. N., Schoenfeld, A. M. and Riley, E. P. (2001) Teratogenic effects of alcohol on brain and behavior. Alcohol Res. Health 25, 185–191.
3 Maier, S. E. and West, J. R. (2001) Regional differences in cell loss associated with binge-like alcohol exposure during the first two trimesters equivalent in the rat. Alcohol 23, 49–57.
4 Minana, R., Climent, E., Barettino, D., Segui, J. M., Renau-Piqueras, J. and Guerri, C. (2000) Alcohol exposure alters the expression pattern of neural cell adhesion molecules during brain development. J. Neurochem. 75, 954–964.
5 Olney, J. W., Ishimaru, M. J., Bittigau, P. and Ikonomidou, C. (2000) Ethanol-induced apoptotic neurodegeneration in the developing brain. Apoptosis 5, 515–521.
6 Swanson, D. J., King, M. A., Walker, D. W. and Heaton, M. B. (1995) Chronic prenatal ethanol exposure alters the normal ontogeny of choline acetyltransferase activity in the rat septohippocampal system. Alcohol Clin. Exp. Res. 19, 1252–1260.
7 Yanni, P. A. and Lindsley, T. A. (2000) Ethanol inhibits development of dendrites and synapses in rat hippocampal pyramidal neuron cultures. Brain Res. Dev. Brain Res. 120, 233–243.
8 Liesi, P. (1997) Ethanol-exposed central neurons fail to migrate and undergo apoptosis. J. Neurosci. Res. 48, 439–448.
9 O'Malley, K. D. and Nanson, J. (2002) Clinical implications of a link between fetal alcohol spectrum disorder and attention-deficit hyperactivity disorder. Can. J. Psychiatry 47, 349–354.
10 Burd, L., Klug, M. G., Martsolf, J. T. and Kerbeshian, J. (2003) Fetal alcohol syndrome: neuropsychiatric phenomics. Neurotoxicol. Teratol. 25, 697–705.
11 Burd, L., Cotsonas-Hassler, T. M., Martsolf, J. T. and Kerbeshian, J. (2003) Recognition and management of fetal alcohol syndrome. Neurotoxicol. Teratol. 25, 681–688.
12 Goodyer, C. G., De, S. L., Lai, W. H., Guyda, H. J. and Posner, B. I. (1984) Characterization of insulin-like growth factor receptors in rat anterior pituitary, hypothalamus, and brain. Endocrinology 114, 1187–1195.
13 Gammeltoft, S., Fehlmann, M. and Van, O. E. (1985) Insulin receptors in the mammalian central nervous system: binding characteristics and subunit structure. Biochimie 67, 1147–1153.
14 Hill, J. M., Lesniak, M. A., Pert, C. B. and Roth, J. (1986) Autoradiographic localization of insulin receptors in rat brain: prominence in olfactory and limbic areas. Neuroscience 17, 1127–1138.
15 Zhang, F. X., Rubin, R. and Rooney, T. A. (1998) Ethanol induces apoptosis in cerebellar granule neurons by inhibiting insulin-like growth factor 1 signaling. J. Neurochem. 71, 196–204.
16 de la Monte, S. M., Neely, T. R., Cannon, J. and Wands, J. R. (2001) Ethanol impairs insulin-stimulated mitochondrial function in cerebellar granule neurons. Cell. Mol. Life Sci. 58, 1950–1960.

17 de la Monte, S. M., Ganju, N., Banerjee, K., Brown, N. V., Luong, T. and Wands, J. R. (2000) Partial rescue of ethanol-induced neuronal apoptosis by growth factor activation of phosphoinositol-3-kinase. Alcohol Clin. Exp. Res. 24, 716–726.

18 Hallak, H., Seiler, A. E., Green, J. S., Henderson, A., Ross, B. N. and Rubin, R. (2001) Inhibition of insulin-like growth factor-I signaling by ethanol in neuronal cells. Alcohol Clin. Exp. Res. 25, 1058–1064.

19 de la Monte, S. M. and Wands, J. R. (2002) Chronic gestational exposure to ethanol impairs insulin-stimulated survival and mitochondrial function in cerebellar neurons. Cell. Mol. Life Sci. 59, 882–893.

20 Ramachandran, V., Perez, A., Chen, J., Senthil, D., Schenker, S. and Henderson, G. I. (2001) In utero ethanol exposure causes mitochondrial dysfunction, which can result in apoptotic cell death in fetal brain: a potential role for 4- hydroxynonenal. Alcohol Clin. Exp. Res. 25, 862–871.

21 Ikonomidou, C., Bittigau, P., Ishimaru, M. J., Wozniak, D. F., Koch, C., Genz, K., Price, M. T., Stefovska, V., Horster, F., Tenkova, T., Dikranian, K. and Olney, J. W. (2000) Ethanol-induced apoptotic neurodegeneration and fetal alcohol syndrome. Science 287, 1056–1060.

22 de la Monte, S. M. and Wands, J. R. (2001) Mitochondrial DNA damage and impaired mitochondrial function contribute to apoptosis of insulin-stimulated ethanol-exposed neuronal cells. Alcohol Clin. Exp. Res. 25, 898–906.

23 de la Monte, S. M., Xu, X. J. and Wands, J. R. (2005) Ethanol inhibits insulin expression and actions in the developing brain. Cell. Mol. Life Sci. 62, 1131–1145.

24 Vander Top, E. A., Wyatt, T. A. and Gentry-Nielsen, M. J. (2005) Smoke exposure exacerbates an ethanol-induced defect in mucociliary clearance of Streptococcus pneumoniae. Alcohol Clin. Exp. Res. 29, 882–887.

25 Maier, S. E., Miller, J. A., Blackwell, J. M. and West, J. R. (1999) Fetal alcohol exposure and temporal vulnerability: regional differences in cell loss as a function of the timing of binge-like alcohol exposure during brain development. Alcohol Clin. Exp. Res. 23, 726–734.

26 Mohamed, S. A., Nathaniel, E. J., Nathaniel, D. R. and Snell, L. (1987) Altered Purkinje cell maturation in rats exposed prenatally to ethanol. I. Cytology. Exp. Neurol. 97, 35–52.

27 Xu, J., Yeon, J. E., Chang, H., Tison, G., Chen, G. J., Wands, J. and de la Monte, S. (2003) Ethanol impairs insulin-stimulated neuronal survival in the developing brain: role of PTEN phosphatase. J. Biol. Chem. 278, 26929–26937.

28 Yeon, J. E., Califano, S., Xu, J., Wands, J. R. and De La Monte, S. M. (2003) Potential role of PTEN phosphatase in ethanol-impaired survival signaling in the liver. Hepatology 38, 703–714.

29 Ausubel, F. M., Brent, R., Kingston, R. E., Moore, D. D., Seidman, J. G., Smith, J. A. and Struhl, K. (2006) Current Protocols in Molecular Biology. John Wiley & Sons, New York.

30 Nikolic, M., Dudek, H., Kwon, Y. T., Ramos, Y. F. and Tsai, L. H. (1996) The cdk5/p35 kinase is essential for neurite outgrowth during neuronal differentiation. Genes Dev. 10, 816–825.

31 Banerjee, K., Mohr, L., Wands, J. R. and de la Monte, S. M. (1998) Ethanol inhibition of insulin signaling in hepatocellular carcinoma cells. Alcohol Clin. Exp. Res. 22, 2093–2101.

32 de la Monte, S. M., Ganju, N. and Wands, J. R. (1999) Microtiter Immunocytochemical ELISA assay: A novel and highly sensitive method of quantifying immunoreactivity. Biotechniques 26, 1073–1076.

33 Fulop, M., Bock, J., Ben-Ezra, J., Antony, M., Danzig, J. and Gage, J. S. (1986) Plasma lactate and 3-hydroxybutyrate levels in patients with acute ethanol intoxication. Am. J. Med. 80, 191–194.

34 Jagger, J., Fife, D., Vernberg, K. and Jane, J. A. (1984) Effect of alcohol intoxication on the diagnosis and apparent severity of brain injury. Neurosurgery 15, 303–306.

35 da Silva, A. M., Payao, S. L., Borsatto, B., Bertolucci, P. H. and Smith, M. A. (2000) Quantitative evaluation of the rRNA in Alzheimer's disease. Mech. Ageing Dev. 120, 57–64.

36 Payao, S. L., Smith, M. A., Winter, L. M. and Bertolucci, P. H. (1998) Ribosomal RNA in Alzheimer's disease and aging. Mech. Ageing Dev. 105, 265–272.

37 Hu, J. G., Fu, S. L., Zhang, K. H., Li, Y., Yin, L., Lu, P. H. and Xu, X. M. (2004) Differential gene expression in neural stem cells and oligodendrocyte precursor cells: a cDNA microarray analysis. J Neurosci. Res. 78, 637–646.

38 Kumagai, T., Kitagawa, Y., Hirose, G. and Sakai, K. (1999) Antibody recognition and RNA binding of a neuronal nuclear autoantigen associated with paraneoplastic neurological syndromes and small cell lung carcinoma. J. Neuroimmunol. 93, 37–44.

39 Szabo, A., Dalmau, J., Manley, G., Rosenfeld, M., Wong, E., Henson, J., Posner, J. B. and Furneaux, H. M. (1991) HuD, a paraneoplastic encephalomyelitis antigen, contains RNA-binding domains and is homologous to Elav and Sex-lethal. Cell 67, 325–333.

40 Imai, Y., Ibata, I., Ito, D., Ohsawa, K. and Kohsaka, S. (1996) A novel gene iba1 in the major histocompatibility complex class III region encoding an EF hand protein expressed in a monocytic lineage. Biochem. Biophys. Res. Commun. 224, 855–862.

41 Ito, D., Tanaka, K., Suzuki, S., Dembo, T. and Fukuuchi, Y. (2001) Enhanced expression of Iba1, ionized calcium-binding adapter molecule 1, after transient focal cerebral ischemia in rat brain. Stroke 32, 1208–1215.

42 Rivera, E., Goldin, A., Fulmer, N., Tavares, R., Wands, J. R. and de la Monte, S. M. (2005) Insulin and insulin-like growth factor expression and function deteriorate with progression of Alzheimer's disease: Link to brain reductions in acetylcholine. J. Alzheimers Dis. 8, 247–268.

43 Cho, C. H., Lee, C. S., Chang, M., Jang, I. H., Kim, S. J., Hwang, I., Ryu, S. H., Lee, C. O. and Koh, G. Y. (2004) Localization of VEGFR-2 and PLD2 in endothelial caveolae is involved in VEGF-induced phosphorylation of MEK and ERK. Am. J. Physiol. Heart Circ. Physiol. 286, H1881–1888.

44 Huo, H., Guo, X., Hong, S., Jiang, M., Liu, X. and Liao, K. (2003) Lipid rafts/caveolae are essential for insulin-like growth factor-1 receptor signaling during 3T3-L1 preadipocyte differentiation induction. J. Biol. Chem. 278, 11561–11569.

45 Meuillet, E. J., Leray, V., Hubert, P., Leray, C. and Cremel, G. (1999) Incorporation of exogenous lipids modulates insulin signaling in the hepatoma cell line, HepG2. Biochim. Biophys. Acta 1454, 38–48.

46 Peiro, S., Comella, J. X., Enrich, C., Martin-Zanca, D. and Rocamora, N. (2000) PC12 cells have caveolae that contain TrkA. Caveolae-disrupting drugs inhibit nerve growth factor-induced, but not epidermal growth factor-induced, MAPK phosphorylation. J. Biol. Chem. 275, 37846–37852.

47 Goodlett, C. R., Horn, K. H. and Zhou, F. C. (2005) Alcohol teratogenesis: mechanisms of damage and strategies for intervention. Exp. Biol. Med. 230, 394–406.

48 Guerri, C. (1998) Neuroanatomical and neurophysiological mechanisms involved in central nervous system dysfunctions induced by prenatal alcohol exposure. Alcohol Clin. Exp. Res. 22, 304–312.

49 Lewis, P. D. (1985) Neuropathological effects of alcohol on the developing nervous system. Alcohol Alcohol 20, 195–200.

50 Ozer, E., Sarioglu, S. and Gure, A. (2000) Effects of prenatal ethanol exposure on neuronal migration, neuronogenesis and brain myelination in the mice brain. Clin. Neuropathol. 19, 21–25.

51 Bandstra, E. S., Morrow, C. E., Anthony, J. C., Accornero, V. H. and Fried, P. A. (2001) Longitudinal investigation of task persistence and sustained attention in children with prenatal cocaine exposure. Neurotoxicol. Teratol. 23, 545–559.

52 Xu, Y. Y., Bhavani, K., Wands, J. R. and de la Monte, S. M. (1995) Ethanol inhibits insulin receptor substrate-1 tyrosine phosphorylation and insulin-stimulated neuronal thread protein gene expression. Biochem. J. 310, 125–132.
53 Dudek, H., Datta, S. R., Franke, T. F., Birnbaum, M. J., Yao, R., Cooper, G. M., Segal, R. A., Kaplan, D. R. and Greenberg, M. E. (1997) Regulation of neuronal survival by the serine-threonine protein kinase Akt. Science 275, 661–665.
54 Kummer, J. L., Rao, P. K. and Heidenreich, K. A. (1997) Apoptosis induced by withdrawal of trophic factors is mediated by p38 mitogen-activated protein kinase. J. Biol. Chem. 272, 20490–20494.
55 Yamaguchi, A., Tamatani, M., Matsuzaki, H., Namikawa, K., Kiyama, H., Vitek, M. P., Mitsuda, N. and Tohyama, M. (2001) Akt activation protects hippocampal neurons from apoptosis by inhibiting transcriptional activity of p53. J. Biol. Chem. 276, 5256–5264.
56 Barres, B. A., Schmid, R., Sendnter, M. and Raff, M. C. (1993) Multiple extracellular signals are required for long-term oligodendrocyte survival. Development 118, 283–295.
57 Barres, B. A., Hart, I. K., Coles, H. S., Burne, J. F., Voyvodic, J. T., Richardson, W. D. and Raff, M. C. (1992) Cell death and control of cell survival in the oligodendrocyte lineage. Cell 70, 31–46.
58 Ness, J. K. and Wood, T. L. (2002) Insulin-like growth factor I, but not neurotrophin-3, sustains Akt activation and provides long-term protection of immature oligodendrocytes from glutamate-mediated apoptosis. Mol. Cell Neurosci. 20, 476–488.
59 Seiler, A. E., Henderson, A. and Rubin, R. (2000) Ethanol inhibits insulin receptor tyrosine kinase. Alcohol Clin. Exp. Res. 24, 1869–1872.
60 Seiler, A. E., Ross, B. N. and Rubin, R. (2001) Inhibition of insulin-like growth factor-1 receptor and IRS-2 signaling by ethanol in SH-SY5Y neuroblastoma cells. J. Neurochem. 76, 573–581.
61 D'Ercole, A. J., Ye, P. and Gutierrez-Ospina, G. (1996) Use of transgenic mice for understanding the physiology of insulin-like growth factors. Horm. Res. 45 Suppl 1, 5–7.
62 D'Ercole, A. J. (1993) Expression of insulin-like growth factor-I in transgenic mice. Ann. N. Y. Acad. Sci. 692, 149–160.
63 Nakae, J., Kido, Y. and Accili, D. (2001) Distinct and overlapping functions of insulin and IGF-I receptors. Endocr. Rev. 22, 818–835.
64 Ghosh, P., Dahms, N. M. and Kornfeld, S. (2003) Mannose 6-phosphate receptors: new twists in the tale. Nat. Rev. Mol. Cell Biol. 4, 202–212.
65 Herr, F., Liang, O. D., Herrero, J., Lang, U., Preissner, K. T., Han, V. K. and Zygmunt, M. (2003) Possible angiogenic roles of insulin-like growth factor II and its receptors in uterine vascular adaptation to pregnancy. J. Clin. Endocrinol. Metab. 88, 4811–4817.
66 Zygmunt, M., McKinnon, T., Herr, F., Lala, P. K. and Han, V. K. (2005) HCG increases trophoblast migration *in vitro* via the insulin-like growth factor-II/mannose-6 phosphate receptor. Mol. Hum. Reprod. 11, 261–267.
67 Patel, T. B. (2004) Single transmembrane spanning heterotrimeric g protein-coupled receptors and their signaling cascades. Pharmacol. Rev. 56, 371–385.
68 Gimpl, G., Burger, K. and Fahrenholz, F. (1997) Cholesterol as modulator of receptor function. Biochemistry 36, 10959–10974.
69 Le Lay, S., Krief, S., Farnier, C., Lefrere, I., Le Liepvre, X., Bazin, R., Ferre, P. and Dugail, I. (2001) Cholesterol, a cell size-dependent signal that regulates glucose metabolism and gene expression in adipocytes. J. Biol. Chem. 276, 16904–16910.
70 Parpal, S., Karlsson, M., Thorn, H. and Stralfors, P. (2001) Cholesterol depletion disrupts caveolae and insulin receptor signaling for metabolic control via insulin receptor substrate-1, but not for mitogen-activated protein kinase control. J. Biol. Chem. 276, 9670–9678.
71 Wu, C., Butz, S., Ying, Y. and Anderson, R. G. (1997) Tyrosine kinase receptors concentrated in caveolae-like domains from neuronal plasma membrane. J. Biol. Chem. 272, 3554–3559.
72 Gustavsson, J., Parpal, S., Karlsson, M., Ramsing, C., Thorn, H., Borg, M., Lindroth, M., Peterson, K. H., Magnusson, K. E. and Stralfors, P. (1999) Localization of the insulin receptor in caveolae of adipocyte plasma membrane. FASEB J. 13, 1961–1971.
73 Cohen, A. W., Combs, T. P., Scherer, P. E. and Lisanti, M. P. (2003) Role of caveolin and caveolae in insulin signaling and diabetes. Am. J. Physiol. Endocrinol. Metab. 285, E1151–1160.
74 Balbis, A., Baquiran, G., Mounier, C. and Posner, B. I. (2004) Effect of insulin on caveolin-enriched membrane domains in rat liver. J. Biol. Chem. 279, 39348–39357.
75 Karlsson, M., Thorn, H., Danielsson, A., Stenkula, K. G., Ost, A., Gustavsson, J., Nystrom, F. H. and Stralfors, P. (2004) Colocalization of insulin receptor and insulin receptor substrate-1 to caveolae in primary human adipocytes. Cholesterol depletion blocks insulin signalling for metabolic and mitogenic control. Eur. J. Biochem. 271, 2471–2479.
76 McGuire, T. F., Xu, X. Q., Corey, S. J., Romero, G. G. and Sebti, S. M. (1994) Lovastatin disrupts early events in insulin signaling: a potential mechanism of lovastatin's anti-mitogenic activity. Biochem. Biophys. Res. Commun. 204, 399–406.
77 Vainio, S., Heino, S., Mansson, J. E., Fredman, P., Kuismanen, E., Vaarala, O. and Ikonen, E. (2002) Dynamic association of human insulin receptor with lipid rafts in cells lacking caveolae. EMBO Rep. 3, 95–100.
78 Podar, K., Tai, Y. T., Cole, C. E., Hideshima, T., Sattler, M., Hamblin, A., Mitsiades, N., Schlossman, R. L., Davies, F. E., Morgan, G. J., Munshi, N. C., Chauhan, D. and Anderson, K. C. (2003) Essential role of caveolae in interleukin-6- and insulin-like growth factor I-triggered Akt-1-mediated survival of multiple myeloma cells. J. Biol. Chem. 278, 5794–5801.
79 Hong, S., Huo, H., Xu, J. and Liao, K. (2004) Insulin-like growth factor-1 receptor signaling in 3T3-L1 adipocyte differentiation requires lipid rafts but not caveolae. Cell Death Differ. 11, 714–723.
80 Kaizer, R. R., Correa, M. C., Spanevello, R. M., Morsch, V. M., Mazzanti, C. M., Goncalves, J. F. and Schetinger, M. R. (2005) Acetylcholinesterase activation and enhanced lipid peroxidation after long-term exposure to low levels of aluminum on different mouse brain regions. J. Inorg. Biochem. 99, 1865–1870.
81 Melo, J. B., Agostinho, P. and Oliveira, C. R. (2003) Involvement of oxidative stress in the enhancement of acetylcholinesterase activity induced by amyloid beta-peptide. Neurosci. Res. 45, 117–127.